CellPress
Partner Journal

Molecular Plant
Research article

Mitigating growth-stress tradeoffs via elevated TOR signaling in rice

Wei Li[1,2,8], Jiaqi Liu[1,8], Zeqi Li[1,3,8], Ruiqiang Ye[4], Wenzhen Chen[1,3], Yuqing Huang[1], Yue Yuan[1], Yi Zhang[1], Huayi Hu[1], Peng Zheng[1,2], Zhongming Fang[5], Zeng Tao[1], Shiyong Song[1], Ronghui Pan[1,2], Jian Zhang[6], Jumim Tu[1], Jen Sheen[7] and Hao Du[1,2,3,*]

[1]State Key Laboratory of Rice Biology, College of Agriculture and Biotechnology, Zhejiang University, Yu-Hang-Tang Road No. 866, Hangzhou 310058, China

[2]ZJU-Hangzhou Global Scientific and Technological Innovation Center, Zhejiang University, Hangzhou 311215, China

[3]Hainan Institute of Zhejiang University, Sanya 572025, China

[4]National Key Laboratory of Plant Molecular Genetics, CAS, Center for Excellence in Molecular Plant Sciences, Shanghai Institute of Plant Physiology and Ecology, Chinese Academy of Sciences, Shanghai 200032, China

[5]Key Laboratory of Plant Resource Conservation and Germplasm Innovation in Mountainous Region (Ministry of Education), College of Agricultural Sciences, Guizhou University, Guiyang 550025, China

[6]State Key Laboratory of Rice Biology and Breeding, China National Rice Research Institute, Hangzhou 311400, China

[7]Department of Molecular Biology and Center for Computational and Integrative Biology, Massachusetts General Hospital, and Department of Genetics, Harvard Medical School, Boston, MA 02114, USA

[8]These authors contributed equally to this article.

***Correspondence: Hao Du (du_hao@zju.edu.cn)**

https://doi.org/10.1016/j.molp.2023.12.002

ABSTRACT

Rice production accounts for approximately half of the freshwater resources utilized in agriculture, resulting in greenhouse gas emissions such as methane (CH_4) from flooded paddy fields. To address this challenge, environmentally friendly and cost-effective water-saving techniques have become widely adopted in rice cultivation. However, the implementation of water-saving treatments (WSTs) in paddy-field rice has been associated with a substantial yield loss of up to 50% as well as a reduction in nitrogen use efficiency (NUE). In this study, we discovered that the target of rapamycin (TOR) signaling pathway is compromised in rice under WST. Polysome profiling-coupled transcriptome sequencing (polysome-seq) analysis unveiled a substantial reduction in global translation in response to WST associated with the downregulation of TOR activity. Molecular, biochemical, and genetic analyses revealed new insights into the impact of the positive TOR-S6K-RPS6 and negative TOR-MAF1 modules on translation repression under WST. Intriguingly, ammonium exhibited a greater ability to alleviate growth constraints under WST by enhancing TOR signaling, which simultaneously promoted uptake and utilization of ammonium and nitrogen allocation. We further demonstrated that TOR modulates the ammonium transporter AMT1;1 as well as the amino acid permease APP1 and dipeptide transporter NPF7.3 at the translational level through the 5′ untranslated region. Collectively, these findings reveal that enhancing TOR signaling could mitigate rice yield penalty due to WST by regulating the processes involved in protein synthesis and NUE. Our study will contribute to the breeding of new rice varieties with increased water and fertilizer utilization efficiency.

Key words: target of rapamycin, TOR, water-saving rice, low-carbon agriculture, drought, nitrogen use efficiency, NUE

Li W., Liu J., Li Z., Ye R., Chen W., Huang Y., Yuan Y., Zhang Y., Hu H., Zheng P., Fang Z., Tao Z., Song S., Pan R., Zhang J., Tu J., Sheen J., and Du H. (2024). Mitigating growth-stress tradeoffs via elevated TOR signaling in rice. Mol. Plant. **17**, 240–257.

INTRODUCTION

With increasing greenhouse gas emissions aggravating global warming, the planet is experiencing rising temperatures and water scarcity. Traditional rice production exacerbates this problem by releasing significant amounts of methane (CH_4), a major greenhouse gas, causing global warming and water shortages in many regions. The flooding of paddy fields, which accounts

Published by the Molecular Plant Shanghai Editorial Office in association with Cell Press, an imprint of Elsevier Inc., on behalf of CSPB and CEMPS, CAS.

for almost 50% of total agricultural water use, produces an anaerobic environment that promotes the decomposition of organic matter and generates CH_4. Additionally, the use of this irrigation mode for rice cultivation leads to fertilizer loss, soil salinization, and water pollution (Li et al., 2006; Zhang et al., 2022b). To tackle these challenges, rice growers have begun transitioning rice cultivation away from flooded conditions, and this has emerged as a highly promising approach to reduce greenhouse gas emissions. Efforts have been made to develop water-saving rice varieties through improved water management and germplasm innovation (Heredia et al., 2022; Xia et al., 2022). However, the widespread adoption of water-saving rice is hindered by its lower yield potential and lower nitrogen use efficiency (NUE). The molecular mechanisms underlying the yield penalties and reduced nitrogen utilization under water-saving conditions are still unknown. Water deficiency in rice paddy fields typically occurs gradually over days to weeks, resulting in decreased crop production and biomass. Insufficient water triggers increased levels of endogenous abscisic acid (ABA) and subsequent stomatal closure. This limits the diffusion rate of CO_2 through mesophyll cells, reducing internal CO_2 availability and hindering photosynthesis (Flexas et al., 2006; Du et al., 2010; Gururani et al., 2015). An adequate water supply is also crucial for plant transpiration, which facilitates nutrient transport from roots to shoots (Cramer et al., 2008; Ouyang et al., 2017). Insufficient water leads to deficient energy production in rice, highlighting a potential tradeoff between water conservation and productivity. Consequently, it has become imperative to comprehend how plants adapt to the declining energy availability in the presence of insufficient water.

The role of target of rapamycin (TOR) as a developmental regulator is widely recognized in both plants and animals. It plays a pivotal role in promoting the upregulation of genes associated with anabolic processes, including mRNA translation and protein, lipid, and cell-wall synthesis, while simultaneously downregulating genes involved in autophagy, stress response, and biomolecule degradation when there is an adequate energy supply (Xiong et al., 2013; Liu and Sabatini, 2020; Li et al., 2021; Mallen-Ponce et al., 2022; Meng et al., 2022). In *Arabidopsis*, the kinase activities of TOR and ribosomal protein S6 (RPS6/eS6) kinase (S6K), the substrate of TOR, are inhibited by cold and osmotic stress (Mahfouz et al., 2006; Wang et al., 2017; Scarpin et al., 2022). In terms of plant responses to drought and osmotic stresses, TOR has been found to be involved in ABA signaling. For instance, when ABA-activated SnRK2s directly interact with and phosphorylate REGULATORY-ASSOCIATED PROTEIN OF TOR (RAPTOR) under conditions of ABA accumulation, TOR activity is inhibited (Wang et al., 2018). This inhibition of TOR activity is a mechanism employed by plants to prioritize survival over growth.

Studies have shown that plants generally prioritize protective stress responses over growth when facing abiotic stresses (Du et al., 2015, 2018; Han et al., 2022). For instance, dehydration treatments reduce the polysomal RNA content and suppress global translation in plants (Kawaguchi et al., 2003, 2004). A recent proteomics study also revealed that water deficiency causes over 40% of leaf total proteins to degrade, which results in a shift toward the free amino acid pool (Heinemann et al., 2021). According to these findings, translational regulation plays a critical role in the response to drought conditions. Proteins and amino acids, which are derived from nitrogen, are intricately connected to amino acid homeostasis and nitrogen uptake, allocation, and utilization (Liu et al., 2022b). These processes enable the rapid provision of vital resources for *de novo* protein synthesis in response to drought. Overall, the regulation of translation and amino acid homeostasis represents critical steps in plant responses to water deficiency, allowing plants to allocate resources toward stress adaptation and survival.

It is well established that drought affects transcriptional regulation. However, the biological basis of the effect of water scarcity on nitrogen assimilation and translational regulation has not been extensively investigated. It has been observed that water deficiency leads to reduced activity of nitrogen-metabolizing enzymes and a decrease in the synthesis of nitrogenous compounds. Interestingly, exogenous nitrogen supplementation has been shown to enhance drought resistance in rice by promoting the developmental plasticity of rice root systems (Tran et al., 2014) as well as improving the photosynthetic machinery and antioxidant capacity (Zhong et al., 2017). Ammonium has been shown to improve rice adaptation to water-scarcity conditions. For example, ammonium is more effective than nitrate in mitigating the negative effects of drought and polyethylene glycol (PEG) treatment on rice growth (Yang et al., 2012; Ding et al., 2015; Cao et al., 2018). Recent studies have highlighted the role of drought and salt tolerance (DST) as a negative osmotic regulator that governs NUE and facilitates the reprogramming of nitrogen utilization in response to drought stress. This regulation occurs through direct control of the rice nitrate reductase gene *NR1.2* by DST (Han et al., 2022). This emphasizes the importance of nitrogen metabolism reprogramming in plant adaptation to drought stress. Although substantial efforts have been made to comprehend transcriptional and post-translational regulation within intricate drought-signaling networks, our understanding of translational modulation in rice under water-saving conditions remains limited. In this study, we made the significant discovery that water-saving treatment (WST) suppresses TOR activity, leading to translational repression of ammonium uptake and nitrogen allocation in rice. Conversely, elevation of TOR signaling dramatically improved biomass and NUE in rice. According to these findings, TOR plays a crucial role in modulating energy homeostasis and productivity in the face of limited water availability.

RESULTS

WST inhibits TOR activity and decreases rice productivity

In our previous research, we discovered that maintaining soil water content (SWC) within the range of 20%–25% triggered a drought escape response in rice, resulting in reduced yield and biomass as a survival strategy (Du et al., 2018). However, the significant yield losses have hindered the widespread adoption of maintaining SWC within 20%–25% in rice production. To achieve a balance between water consumption and yield, researchers have developed water-saving strategies for growing water-saving and drought-resistant rice (WDR), with the aim of significantly reducing water usage and greenhouse gas emissions (Xia et al., 2022). However, this strategy still leads to a significant decrease in yield in elite rice varieties, and

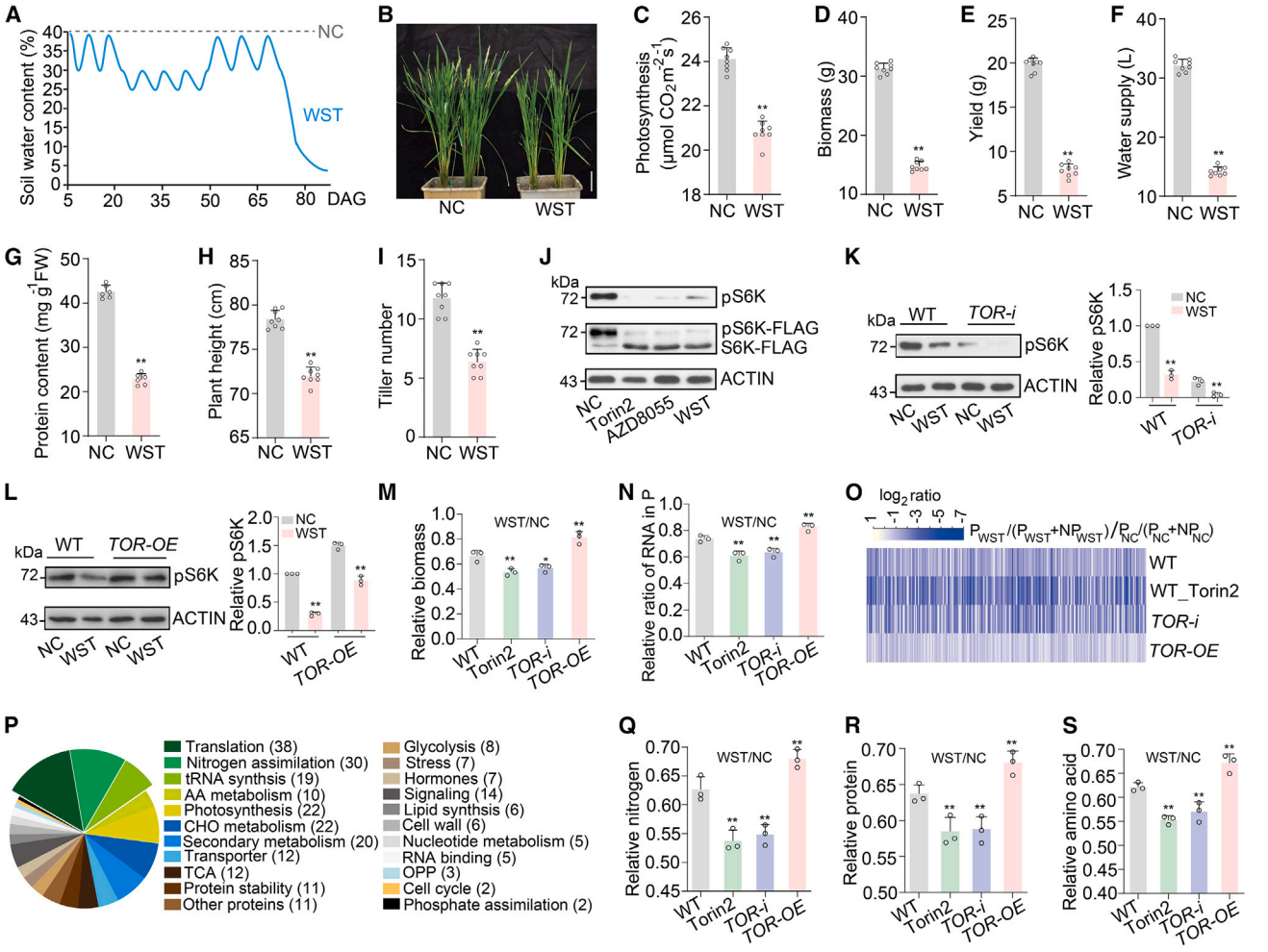

Figure 1. TOR signaling regulates protein translation under WST in rice.

(A) Schematic design of the water-saving treatment (WST) for paddy-field rice cultivation during the entire duration of growth. The blue line indicates soil water content for the WST (described in methods), and the gray dotted line indicates soil water content under the normal condition (NC). DAG, days after germination.

(B) Performance of paddy-field rice under NC and WST; photograph was taken at 70 DAG. Scale bar, 10 cm.

(C) Photosynthesis rate of seedlings at 35 DAG. Error bars indicate means ± SD (n = 8). Statistical significance was assessed using two-tailed t-tests. $^{**}p < 0.01$.

(D and E) Above-ground dry biomass and yield per plant under NC and WST conditions. Error bars indicate means ± SD (n = 8). Statistical significance was assessed using two-tailed t-tests. $^{**}p < 0.01$.

(F) Statistical data of the water supply per plant throughout the entire growth period. Error bars indicate means ± SD (n = 8). Statistical significance was assessed using two-tailed t-tests. $^{**}p < 0.01$.

(G) Measurement of protein content of rice seedlings at 35 DAG. Error bars represent means ± SD (n = 6). Statistical significance was assessed using two-tailed t-tests. $^{**}p < 0.01$.

(H and I) Plant height **(H)** and tiller number **(I)** of WT rice under NC or WST. Error bars indicate means ± SD (n = 8). Statistical significance was assessed using two-tailed t-tests. $^{**}p < 0.01$.

(J) WST repression of TOR activity *in vivo* revealed by immunoblot analyses. Protein from rice *S6K1-OE* seedlings detected by anti-FLAG antibody (Sigma, F1804) after treatment. The upper band indicates phosphorylated S6K1. TOR inhibitors (Torin2 and AZD8055) at a concentration of 10 μM were spread on the leaves of 28-day rice for 7 days, and leaves were sampled at 35 DAG. TOR activation was also confirmed using an anti-phospho antibody of S6K1 (Agrisera, AS132664).

(K and L) TOR activity is relevant to TOR expression levels in WT, *TOR-i* (RNA interference) **(K)**, and *TOR-OE* rice **(L)**. Quantification of pS6K intensity from western blot analysis with three repeats.

(M) Relative above-ground biomass of rice after 7-day WST treatment. Error bars indicate means ± SD (n = 3). Statistical significance was assessed using two-tailed t-tests. $^{**}p < 0.01$.

(N) Bar graph shows the ribosome-loading efficiency presented as the ratio of P (polysomal) RNA to the sum of total P and NP (non-polysomal) RNAs after 7-day WST treatment. RNA in polysomes % = (amount of P RNA/amount of both P and NP RNA) × 100%. Error bars indicate means ± SD (n = 3). Statistical significance was assessed using two-tailed t-tests. $^{**}p < 0.01$.

(legend continued on next page)

the biological mechanism underlying this decrease remains unclear.

To investigate the molecular mechanisms underlying the significant yield reduction under water-saving conditions in rice, we implemented WST, which is commonly used for WDR, for growing the japonica rice variety *Kitaake* (Figure 1A) and observed a substantial decrease in photosynthesis rate, tiller number, plant height, biomass, and yield associated with the decrease in water supply during WST (Figure 1B–1I). According to a previous proteomics study on drought-treated *Arabidopsis*, water deficiency leads to a reduced accumulation of leaf proteins required for drought adaptation (Heinemann et al., 2021). This prompted us to investigate protein content, which forms the foundation for plant structure and biological enzyme activity, in whole plants. Our findings revealed a significant decrease in the accumulation of total protein under WST (Figure 1G), suggesting a potential reduction in protein translation following WST.

The evolutionarily conserved TOR signaling pathway is known to play a crucial role in regulating protein synthesis. To investigate the effects of WST on endogenous TOR kinase activity, we utilized a well-established method to immunologically detect the phosphorylation of S6K1, a canonical TOR substrate, in plants using a phospho-specific antibody (Xiong and Sheen, 2012; Ye et al., 2022). In rice, some studies have provided indirect evidence of S6K1 phosphorylation by TOR (Sun et al., 2016; Bakshi et al., 2023). A conserved phosphorylation site (S465) was identified in the FxxFT/SYVxP motif of rice S6K1 (Xiong and Sheen, 2012) (Supplemental Figure 1). We transiently expressed S6K1-FLAG in rice protoplasts and selected optimal transgenic rice plants stably expressing S6K1-FLAG for more extensive analyses (Xiong and Sheen, 2012) (Supplemental Figure 2). We conducted *in vivo* pS6K phosphorylation analysis, co-immunoprecipitation, and *in vitro* kinase assays, and confirmed TOR regulation of pS6K1, the physical interaction between TOR and S6K1, and the direct phosphorylation of S6K1 by TOR (Figure 1J and Supplemental Figure 2B–2D). Our results support the high conservation of TOR-S6K signaling in plants and animals.

To further understand the molecular mechanism of rice TOR-S6K signaling under WST, we conducted experiments using rice *S6K1* overexpression (*S6K1-OE*) lines and treated them with WST or TOR inhibitors (Figure 1J and Supplemental Figure 2A). The results demonstrated significant repression of TOR activity by WST, suggesting that TOR may be related to the adaptive changes of rice under WST. Subsequently, we created *TOR* RNA interference (hereafter referred to as *TOR-i*) and *TOR* overexpression (*TOR-OE*) transgenic lines in the *Kitaake* background and confirmed the presence of the transgenes using quantitative reverse-transcription PCR (qRT–PCR) and immunoblot analyses (Supplemental Figure 3A–3C). Phenotyping analysis of TOR genetic materials revealed that higher TOR activity promoted growth height and tillering, and resulted in higher yield and biomass (Supplemental Figure 3D–3G). Based on immunoblot analysis, TOR activity was relatively low in *TOR-i* lines, and WST further suppressed TOR activity in these plants (Figure 1K). Conversely, TOR exhibited higher kinase activity compared to the wild type (WT) under both normal conditions and WST in *TOR-OE* plants (Figure 1L). We then investigated whether TOR activity was critical for growth under WST. To eliminate any developmental effects of transgenic rice, we present our data as relative biomass (for raw data, see Supplemental Table 3). It was evident that *TOR-i* and Torin2-treated seedlings accumulated less relative biomass (Figure 1M), whereas *TOR-OE* seedlings had larger relative biomass even under WST (Figure 1M). Based on these findings, TOR enhances plant growth and alleviates the growth retardation caused by WST.

WST suppresses TOR-regulated protein translation

It is well known that TOR plays a crucial role in translational regulation. Previous ribosome profiling studies have shown that TOR controls the translation of various transcripts (Lee et al., 2017; Chen et al., 2018; Scarpin et al., 2020). Using a similar ribosome profiling approach, we observed a significant shift in RNA distribution from polysomal (P) to non-polysomal (NP) fractions after WST in WT seedlings (Figure 1N and Supplemental Figure 4A). *TOR-i* and Torin2-treated seedlings showed reduced levels of P RNA, while *TOR-OE* seedlings displayed a higher ratio of P RNA after WST (Figure 1N and Supplemental Figure 4A). This suggested that the repression of mRNA translation under WST is linked to TOR activity. To gain a better understanding of the translational networks involved in the TOR signaling pathway under WST, we performed polysome profiling and subsequent RNA sequencing (RNA-seq) analyses. After rigorous statistical analysis and filtering, we identified mRNAs encoded by 274 genes that were co-repressed by WST and low TOR activity conditions, and this repression was significantly alleviated in *TOR-OE* seedlings (Figure 1O and Supplemental Table 2). The wide range of mRNA translation changes indicated that TOR may modulate various essential cellular and metabolic functions repressed by WST (Figure 1O and Supplemental Table 2). The most significantly enriched functional classes of mRNAs/genes included those involved in translation, nitrogen utilization, tRNA synthesis, amino acid metabolism, photosynthesis, carbohydrate metabolism, secondary metabolism, transporters, glycolysis, the tricarboxylic acid cycle, protein degradation, stress responses, signaling, and transcription (Figure 1P and Supplemental Table 2). Importantly, 87 WST-repressed mRNAs involved in conserved translation and nitrogen utilization were correlated with TOR activity (Figure 1O

(O) Hierarchical clustering analysis of TOR signaling under WST-repressed transcriptome enrichment in polysomal (P; fractions 9–14) mRNA and non-polysomal (NP; fractions 1–7) mRNA. Analysis of the translatome experiments by comparing the mRNA associated with polysomes to the mRNA from NP fractions. Each sample was from 15 seedlings collected at 35 DAG after 7-day WST or 7-day 10 μM Torin2 treatments. P_{WST} indicates mRNA associated with polysomes after WST, NP_{WST} indicates mRNA associated with non-polysomes after NC. WST, water-saving treatment; NC, normal conditions. Raw data are provided in Supplemental Table 2.
(P) MapMan functional categories for TOR signaling genes under WST in Figure 1O; for raw data, see Supplemental Table 2.
(Q–S) Physiological measurements of relative nitrogen content **(Q)**, protein content **(R)**, and amino acid content **(S)** in rice at 35 DAG. Error bars indicate means ± SD ($n = 3$). Statistical significance was assessed using two-tailed *t*-tests. $^{**}p < 0.01$.

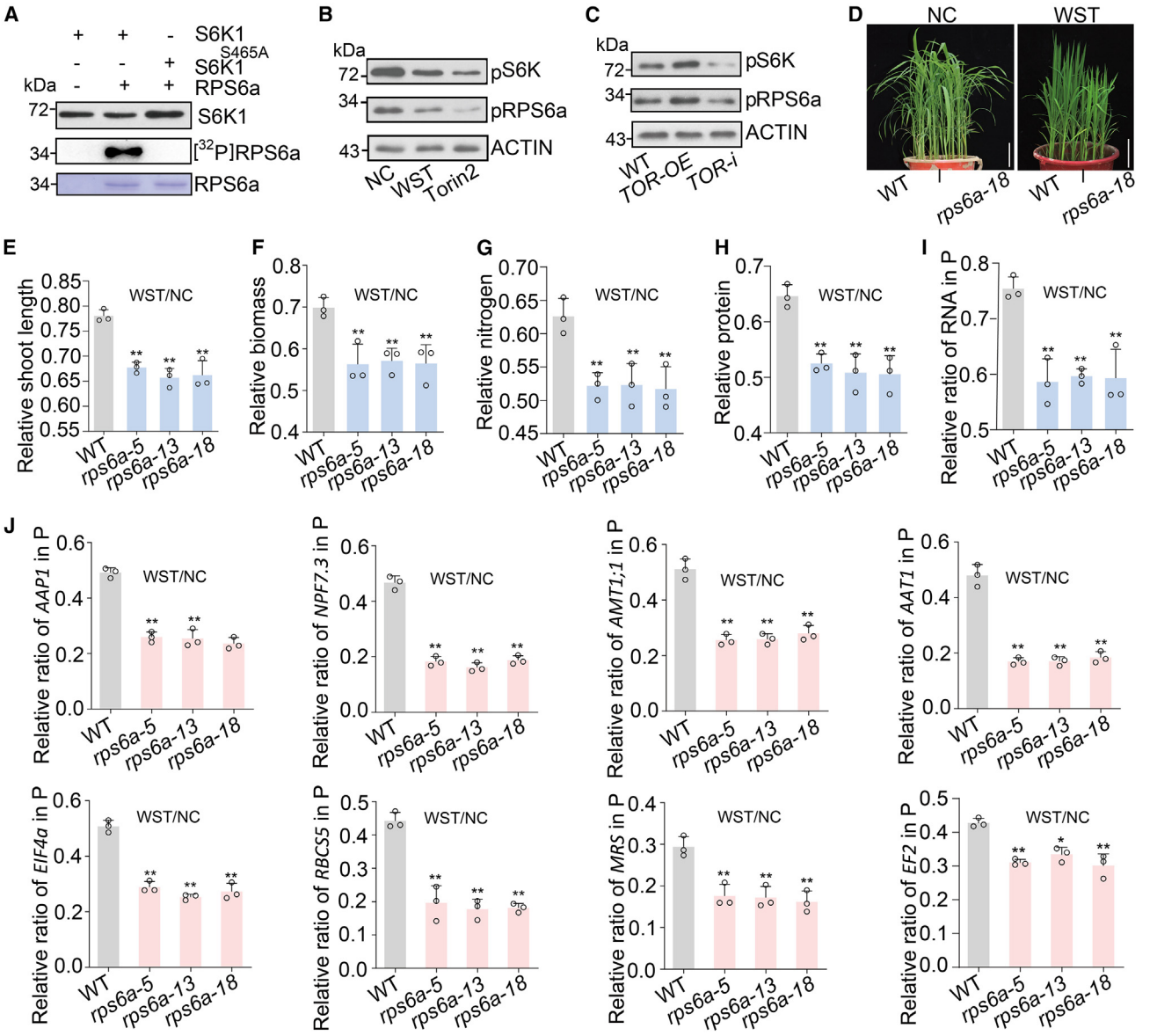

Figure 2. The rice TOR-S6K1-RPS6a module is involved in WST-mediated repression of polysomal mRNA accumulation.

(A) S6K1 directly phosphorylates RPS6a/es6, as shown using an *in vitro* kinase assay. The activity of S6K1 is abolished in S6K1^{S465A}.

(B) Activation of RPS6a is dependent on TOR activity *in vivo*, as shown using phospho-RPS6 and phospho-S6K antibodies. Torin2 (10 μM) was spread on the leaves of 28-day rice for 7 days, and leaves were sampled at 35 DAG.

(C) Phosphorylation of RPS6a is dependent on TOR activity in *TOR-OE* and *TOR-i* rice at 35 DAG *in vivo*. RPS6a phosphorylation and TOR activity were detected using hosphor-RPS6 and hosphor-S6K antibodies, respectively.

(D–F) Impaired growth performance **(D)** revealed by measurements of relative shoot length **(E)** and relative biomass **(F)** of rice *rps6a* mutants under 7-day WST at 35 DAG. Error bars indicate means ± SD (n = 3). Statistical significance was assessed using two-tailed t-tests. $^{**}p < 0.01$. Scale bar, 5 cm.

(G and H) Reduced relative nitrogen **(G)** and relative protein **(H)** contents in rice *rps6a* mutants after 7-day WST. Error bars indicate means ± SD (n = 3). Statistical significance was assessed using two-tailed t-tests. $^{**}p < 0.01$.

(I) Bar graph shows the ratio of ribosome-loading efficiency for WT and the *rps6a* mutant. RNA in polysomes % = (amount of P RNA/amount of P and NP RNA) × 100%. Error bars indicate means ± SD (n = 3). Statistical significance was assessed using two-tailed t-tests. $^{**}p < 0.01$.

(J) Polysomal distribution of specific mRNA transcripts in WT and *rps6a* mutants grown under NC and 7-day WST conditions. The relative expression level of genes in polysomes was calculated as the percentage of the amount of gene expression to the amount of total RNA (P + NP). *ACTIN* was used to normalize the data. Error bars indicate means ± SD (n = 3). Statistical significance was assessed using two-tailed t-tests. $^{*}p < 0.05$, $^{**}p < 0.01$.

and 1P; Supplemental Table 2), highlighting the importance of the dynamic TOR activity-mediated translatome in the context of WST-growth tradeoffs. The data presented above suggested that WST inhibits the accumulation of specific proteins associated with TOR activity.

To ensure accurate calibration of mRNAs isolated from total polysomes and non-polysomes, we used the control *ACTIN* mRNA together with the *RBCS5* (Rubisco small subunit) mRNA and RT–PCR to demonstrate the specific dynamic changes associated with TOR and WST (Supplemental

Figure 4B). To further validate the enriched functional categories, we conducted qRT–PCR assays to quantify the abundance of selected marker mRNAs in non-polysomes and polysomes. Six mRNAs of well-characterized genes, namely *AAT1* (alanine aminotransferase 1), *EIF4a* (eukaryotic initiation factor 4a), *EF2* (elongation factor 2), *RPS6a*/*eS6* (ribosomal protein S6a), the tRNA synthesis gene *MRS* (methionyl-tRNA synthetase), and the photosynthesis gene *RBCS5*, were selected for qRT–PCR analysis using samples from P fractions and purified mRNAs. We observed that the relative mRNA abundance of these genes in polysomes was reduced in WT rice treated with Torin2 and in *TOR-i* rice plants. Conversely, these genes in *TOR-OE* seedlings showed an increase in relative mRNA abundance in polysomes under WST (Supplemental Figure 4C). These findings suggested that the decrease in translation is associated with reduced TOR activity caused by WST or Torin2 treatment. Thus, we confirmed that the translational repression induced by WST is correlated with TOR activity and that overexpressing TOR can alleviate this repression.

The TOR signaling pathway has been shown to regulate both global translation levels and the translation of individual transcripts in plants (Merchante et al., 2017; Chen et al., 2018; Schepetilnikov and Ryabova, 2018; Scarpin et al., 2020, 2022). This led us to investigate whether the TOR signaling pathway regulates the accumulation of nitrogen, protein, and amino acids in rice under WST. Our physiological measurements showed that the relative total nitrogen, protein, and amino acid contents in WT rice decreased to approximately 63%, 64%, and 61%, respectively, after WST (Figure 1Q–1S). Interestingly, rice treated with Torin2 and *TOR-i* seedlings exhibited significantly lower levels of relative nitrogen, protein, and amino acids under WST (Figure 1Q–1S). In contrast, *TOR-OE* rice with relatively higher TOR activity after WST treatment accumulated relatively more nitrogen, protein, and amino acids (Figure 1Q–1S). In addition, specific mRNAs related to nitrogen uptake, allocation, utilization, and translation accumulated in the P fractions of TOR-OE rice after WST (Figure 1O and 1P). These clues suggested that TOR may alleviate growth repression caused by WST by enhancing the translation of proteins involved in nitrogen uptake and allocation.

WST inhibits translation regulated by TOR-S6K-RPS6 signaling

Recent studies have provided evidence suggesting that RPS6/eS6 plays a crucial role in regulating translation and that it is phosphorylated by TOR-S6K signaling under diverse conditions (Chen et al., 2018; Bakshi et al., 2023; Nguyen et al., 2023). To gain a better understanding of how S6K-RPS6 signaling pathways affect translation under WST in rice, we selected the *RPS6* paralog in the rice genome, *RPS6a*, which share a conserved protein sequences with other eukaryotes as the research object (Supplemental Figure 5). Through an *in vitro* kinase assay using RPS6a protein purified from *Escherichia coli*, we confirmed that RPS6a is a direct substrate of S6K1 (Figure 2A). Next, we examined whether RPS6 is differentially phosphorylated in rice seedlings in response to changes in TOR activity. Total proteins were isolated from 35-day-old seedlings treated with WST or Torin2 for 6 h and subjected to immunoblot analyses. The results showed that the phosphorylation of rice RPS6a was reduced by WST or Torin2 treatment (Figure 2B). By enhancing RPS6a activity by overexpressing *TOR* and inhibiting its activity in *TOR-i* rice, we further confirmed that RPS6a activity is positively regulated by TOR-S6K signaling (Figure 2C). This suggests that WST led to the inhibition of RPS6 and highlights the dependence of RPS6 activity on TOR.

To investigate the function of rice RPS6 in TOR signaling under WST, we created *rps6a* mutants using the CRISPR-Cas9 tool (Supplemental Figure 6A and 6B). Under normal conditions, the *rps6a* mutants showed a similar phenotype to the WT at the seedling stage (Figure 2D). However, under WST, the *rps6a* mutants displayed relatively shorter shoot lengths and less biomass (Figure 2D–2F), indicating that RPS6 is an essential growth regulator during WST. However, it should be noted that reduced RPS6 accumulation in the *Arabidopsis* knockout mutants *rps6a* or *rps6b* resulted in a slower growth phenotype at the seedling and adult stages (Creff et al., 2010; Ren et al., 2012). This observation suggests divergence in the role of RPS6 between monocots and dicots. In yeast, deletion of the *RPS6B* gene significantly extends replicative lifespan by modulating translation, which alters the aging process (Chiocchetti et al., 2007). Importantly, the function of rice RPS6, particularly under water deficiency, is still largely unknown.

We found that during the reproductive stage, rice plants with defects in *RPS6a* exhibit dramatically reduced plant height but not tiller number (Supplemental Figure 6C–6E). This suggested that although rice RPS6a and RPS6b have nearly identical protein sequences, RPS6a plays an indispensable role in growth, especially under WST. In terms of translational regulation, previous studies have shown that the rate of protein synthesis of the reporter gene *GUS* is higher in plants overexpressing *TOR* or *RPS6a*/*b* but lower in *tor* and *rps6* mutants (Ren et al., 2012). Building upon the findings related to rice *rps6a* mutants described in Figure 2D–2F, and the biological function of RPS6 in protein translation, we examined whether the morphological changes induced by WST were associated with nitrogen accumulation and protein synthesis. A significant decrease in the relative levels of nitrogen and protein was observed under WST in *rps6a* mutants (Figure 2G and 2H). To further explore the impact of RPS6a on translation under WST, we isolated P RNA from *rps6a* mutant leaves and performed RT–PCR assays. We observed a significant decrease in the relative ratio of P RNA in the *rps6a* mutants under WST compared with WT (Figure 2I and Supplemental Figure 6F). Additionally, we examined the relative ratio of specific mRNAs from polysomes in the *rps6a* mutants, which indicated that WST reduced the content of translation-related mRNAs in P RNA of rice *rps6a* mutants, such as *AAT1*, *EIF4a*, *EF2*, *RPS6a*/*eS6*, *MRS*, and *RBCS5* as well as nitrogen transporters, *AAP1* (amino acid permease 1), *NPF7.3*/*OsPTR6* (dipeptide transporter), and *AMT1;1* (ammonium transporter 1;1) (Figure 2J and Supplemental Figure 6G). Overall, these findings support the involvement of the TOR-S6K-RPS6 module in regulating protein translation, particularly under WST.

TOR repression of MAF1 promotes tRNA synthesis

MAF1 is a conserved repressor of RNA polymerase III (RNA Pol III), and affects protein translation by controlling the biosynthesis

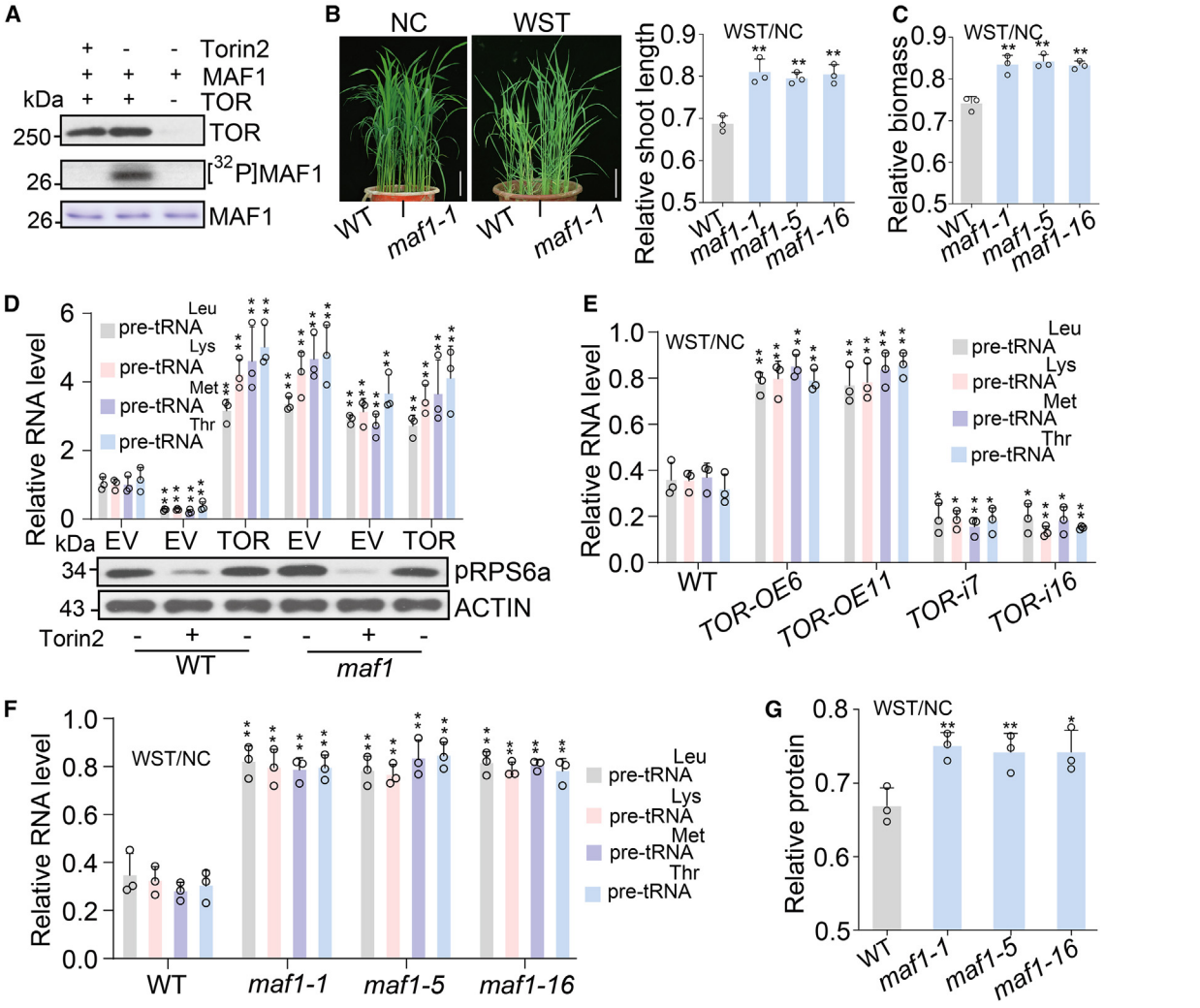

Figure 3. TOR repression of MAF1 modulates tRNA biosynthesis *in vivo*.

(A) TOR directly phosphorylates rice MAF1 protein, as determined by *in vitro* kinase assay.

(B and C) Rice *maf1* mutants show relatively longer shoots **(B)** and higher above-ground biomass **(C)** after 7-day WST. There were three biological repeats, and measurements were taken at 35 DAG. Scale bar, 5 cm. Statistical significance was assessed using two-tailed *t*-tests. $^{**}p < 0.01$. Scale bar, 5 cm.

(D) TOR promotes the biosynthesis of pre-tRNAs (Leu, Lys, Met, Thr) in protoplasts from WT and *maf1* mutants. Protoplasts were harvested after transfection or after 10 μM Torin2 treatment for 6 h. TOR activity was determined by measuring the level of phosphorylated RPS6a in immunoblot analyses. Error bars indicate means ± SD ($n = 3$). Statistical significance was assessed using two-tailed *t*-tests. $^{**}p < 0.01$.

(E and F) qPCR analyses of the relative level of pre-tRNAs (Leu, Lys, Met, Thr) in WT and *maf1* mutants **(E)** and in *TOR-i* and *TOR-OE* rice **(F)**. Error bars indicate means ± SD ($n = 3$). Statistical significance was assessed using two-tailed *t*-tests. $^{*}p < 0.05$, $^{**}p < 0.01$.

(G) Relative total protein content in *maf1* mutant and WT rice seedlings. Error bars indicate means ± SD ($n = 3$). Statistical significance was assessed using two-tailed *t*-tests. $^{*}p < 0.05$, $^{**}p < 0.01$.

of tRNAs in eukaryotes (Khanna et al., 2015). It has been shown that MAF1 predominantly binds to RNA Pol III and functions as a repressor to suppress cell growth (Ahn et al., 2019; Oliveira Andrade et al., 2020). Under conditions that promote growth and involve higher TOR activity, MAF1-mediated transcriptional repression can be relieved (Willis and Moir, 2007; Kantidakis et al., 2012). However, the biological mechanism of MAF1's function in plants under WST remains unclear. Since WST represses TOR activity and mRNA translation, we aimed to investigate whether the negative-acting TOR-MAF1 module is involved in the decreased protein levels observed under WST (Figure 2B).

Amino acid sequence alignment revealed a high degree of conservation of the MAF1 sequence in eukaryotes (Supplemental Figure 7). While previous studies have indicated that mammalian MAF1 is phosphorylated by mammalian TOR complex 1 (mTORC1) rather than mTORC2 (Michels, 2011), the phosphorylation of MAF1 by TOR remains a topic of controversy. To this end, we performed kinase assays *in vitro* and directly demonstrated that MAF1 can function as a substrate of TOR in rice (Figure 3A). To further elucidate the function of rice MAF1 under WST, we generated *maf1* mutants in rice using the CRISPR-Cas9 system (Supplemental Figure 8A). Under normal growth conditions, the *maf1* mutants

exhibited increased plant height but significantly lower fertility (Supplemental Figure 8B–8F), indicating that the *maf1* mutants exhibited stronger growth productivity but at a notable fertility cost. This performance was comparable to the modest growth advantage observed in *Arabidopsis MAF1 RNAi* lines (Blayney et al., 2022). Interestingly, the rice *maf1* mutants displayed relatively greater shoot length and above-ground biomass compared to the WT under WST (Figure 3B and 3C), suggesting that MAF1 modulates the growth process, probably through the RNA Pol III pathway.

To investigate the association between tRNA synthesis and direct regulation by the TOR-MAF1 module, we transfected protoplasts from WT and *maf1* mutants with an empty vector or one expressing TOR and then treated them with or without Torin2 for 6 h. The transcript levels of pre-tRNAs were subsequently measured. We observed that pre-tRNAs accumulated in protoplasts with higher TOR activity (Figure 3D). However, in the *maf1* mutants, TOR had a limited effect on promoting pre-tRNA synthesis (Figure 3D), confirming that TOR regulates tRNA synthesis through MAF1. To evaluate the impact of TOR and MAF1 on pre-tRNA biogenesis, we conducted qRT–PCR analysis using total small RNAs extracted from *TOR* transgenic seedlings and *maf1* mutants and found that the transcript levels of pre-tRNAs significantly decreased under WST (Figure 3E and 3F). In contrast, *TOR-OE* seedlings and the *maf1* mutants exhibited relatively higher levels of pre-tRNAs compared to the WT and *TOR-i* seedlings after WST (Figure 3E and 3F). These results suggested that MAF1 plays a role in modulating tRNA biogenesis, which is dependent on TOR activity. To investigate whether the *maf1* mutants exhibited alterations in protein synthesis in response to the repression caused by WST, we examined the relative protein contents in the *maf1* mutants and WT. Interestingly, we observed higher relative protein contents in the *maf1* mutants compared to WT under WST conditions (Figure 3G). Considering that *TOR-OE* rice exhibited relatively high accumulation of protein and amino acids, which would lead to better growth performance, these findings further support the role of TOR-MAF1 in promoting tRNA synthesis and transfer of amino acids to the translational machinery. Our data demonstrated that the TOR-MAF1 module regulates the synthesis of pre-tRNAs under WST. Moreover, the overexpression of TOR in rice leads to the inhibition of MAF1 through phosphorylation. This, in turn, enhances tRNA biogenesis and subsequent protein synthesis, ultimately conferring resistance to growth retardation.

TOR regulates the translation of mRNAs associated with nitrogen uptake and allocation

Our analysis of polysome profiling and transcriptome data showed that the TOR signaling pathway regulates the mRNAs critical for nitrogen uptake and allocation under WST (Figure 1O and 1P; Supplemental Table 2). We also observed a correlation between TOR activity and relative levels of total nitrogen, protein, and amino acids in rice (Figure 1Q–1S). Previous studies have demonstrated that plants primarily take up nitrogen from the soil through various transport systems, including inorganic ammonium (NH_4^+) and organic forms such as amino acids and peptides (Tegeder and Masclaux-Daubresse, 2018; Liu et al., 2022a). Based on our polysome profiling results, the translation of *AAP1*, *NPF7.3/OsPTR6*, and *AMT1;1* mRNAs was inhibited under WST (Figure 1O and Supplemental Table 2). These three genes have been shown to enhance rice yield by improving NUE (Fan et al., 2014; Li et al., 2016; Ji et al., 2020; Wu et al., 2022). However, it remains unclear whether they are involved in nitrogen uptake and allocation under water-saving conditions and whether TOR regulates these processes.

To investigate this, we transfected protoplasts isolated from the sheaths of 15-day-old WT and *TOR-OE* rice seedlings with hemagglutinin (*HA*)-tagged genomic sequences of *AAP1*, *NPF7.3*, and *AMT1;1* (Supplemental Figure 9A). The transfected protoplasts were then incubated in a W5 solution containing 10 μM TOR inhibitor (Torin2 or AZD8055) for 6 h. The protoplasts were then harvested for immunoblot analysis using an anti-HA antibody to detect the nascent synthesized proteins from the artificial constructs (Figure 4A and 4C; Supplemental Figure 9A). Concurrently, we conducted a qRT–PCR assay to examine the *de novo* transcription of mRNAs using primers targeting the gene body and the *HA* tag (Figure 4B and 4D; Supplemental Figure 9A). To more accurately assess the effect of TOR on the translation of specific mRNAs, we calculated the ratio of nascent synthesized protein to transcriptional mRNA, which serves as a measure of the translational efficiency of *AAP1*, *NPF7.3*, and *AMT1;1*. Based on the relative intensity of the signal, the level of *de novo* synthesis of the AAP1, NPF7.3, and AMT1;1 proteins was significantly lower, approximately only 20%–30% of the control, in the protoplasts with inhibited TOR activity (Figure 4A and 4B). In contrast, the abundance of nascent synthesized mRNAs was 2–3 times higher in *TOR-OE* rice compared to WT (Figure 4C and 4D), indicating that TOR promotes the translation of the AAP1, NPF7.3, and AMT1;1 proteins from their mRNAs in protoplasts, implying that TOR may participate in regulating nitrogen uptake and allocation at the translational level in rice.

To further explore the role of TOR signaling in controlling the translation of AAP1, NPF7.3, and AMT1;1 in plants, we treated rice seedlings with TOR inhibitors as described earlier. P RNA was extracted following ribosome isolation for subsequent RT–PCR assays. To establish a control, total mRNA from lysed cells was used. The results demonstrated a significant reduction in *AAP1*, *NPF7.3*, and *AMT1;1* transcripts from P mRNAs when TOR activity was inhibited in rice (Figure 4E). To genetically confirm the regulation of AMT1;1 translation in WST by TOR signaling, we utilized a commercial anti-AMT1;1 antibody to detect endogenous AMT1;1 protein accumulation in rice. Although the transcript levels did not exhibit a significant decrease in response to altered TOR activity (Supplemental Figure 9B), we observed a notably low abundance of *AMT1;1* mRNA in polysomes from seedlings with reduced TOR activity (Figure 4E), indicating that the reduced ribosome-loading efficiency of AMT1;1 mRNAs is associated with suppressed TOR activity. Next, we performed immunoblot analyses to assess the protein abundance of AMT1;1 in rice treated with WST or Torin2. The results revealed a decrease in the accumulation of AMT1;1 protein, consistent with decreased TOR activity (Figure 4F). Furthermore, we examined the AMT1;1 protein level in *TOR-OE* rice with or without WST. Interestingly, immunoblot analysis demonstrated that enhanced TOR activity led to an increase in AMT1;1 protein accumulation in rice, particularly under WST conditions (Figure 4G), despite the absence of a significant increase in transcript levels (Supplemental Figure 9C). These findings prompted us to investigate whether the translation of

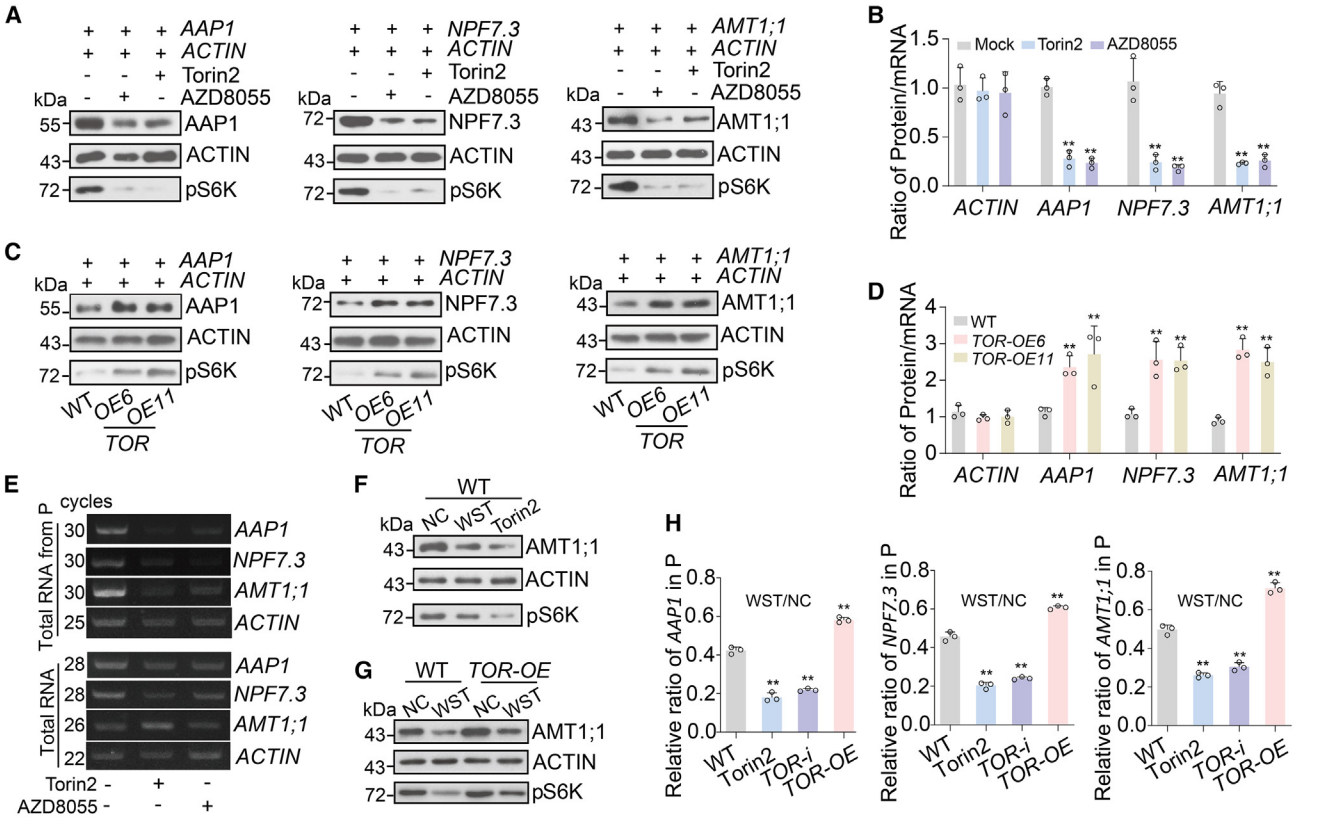

Figure 4. TOR regulates the translation of AAP1, NPF7.3, and AMT1;1 in rice under WST.

(A–D) TOR promotes *de novo* protein synthesis of AAP1, NPF7.3, and AMT1;1 in rice protoplasts. Protoplasts were treated with a TOR inhibitor (10 μM Torin2 or AZD8055) as a negative control. The ratios of protein/mRNA levels **(B and D)** were calculated using mRNA and protein levels obtained from qPCR and western blot assays **(A and C)**, respectively. Quantification of the band intensities in the protein blot were performed using Image Lab (Bio-Rad). The relative value of each band represents the ratio of band intensity to the loading control intensity. qRT–PCR assays of the transcripts of *ACTIN*, *AAP1*, *NPF7.3*, and *AMT1;1* from constructs, primers across specific target genes, and HA tags are shown in Supplemental Figure 9. *ACTIN* was used as a reference gene. Error bars indicate means ± SD ($n = 3$). Statistical significance was assessed using two-tailed *t*-tests. $^{**}p < 0.01$.

(E) RT–PCR analysis of the transcripts of *ACTIN*, *AAP1*, *NPF7.3*, and *AMT1;1* from rice seedlings at 35 DAG after 7-day treatment with 10 μM Torin2 or AZD8055. Expression levels in total mRNA were determined from quantified polysomal (P) mRNA after ribosome extraction and total RNA before ribosome extraction. *Actin* was used as an internal control.

(F and G) *In vivo* immunoblot analyses of AMT1;1 in WT **(F)** and *TOR*-overexpressing transgenic rice **(G)** under WST or 10 μM Torin2 treatment at 35 DAG.

(H) TOR promotes protein synthesis of AAP1, NPF7.3, and AMT1;1 *in vivo*, as determined by polysome profiling-coupled qRT–PCR assays of the *AAP1*, *NPF7.3*, and *AMT1;1* transcripts in polysomal (P) mRNA. Total mRNA was extracted from P mRNA, followed by cDNA synthesis and qRT–PCR using gene-specific primers. The abundance of specific mRNA in P mRNA was quantified as the relative level in polysomes using *ACTIN* as a reference gene. Error bars indicate means ± SD ($n = 3$). Statistical significance was assessed using two-tailed *t*-tests. $^{**}p < 0.01$.

these mRNAs was regulated by WST-TOR signaling directly. Using a combination of polysome profiling and qRT–PCR, we examined the ratio of these mRNAs in polysomes. The results showed that the low TOR activity in *TOR-i* seedlings and Torin2-treated seedlings reduced the translation of these mRNAs (Figure 4H). Interestingly, overexpressing *TOR* alleviated the inhibitory effect of WST and led to the accumulation of more target mRNAs in polysomes (Figure 4H). Collectively, these findings indicated that TOR signaling enhances translation of specific mRNAs associated with nitrogen uptake and allocation, which affects as vitality of rice under water-saving conditions.

TOR enhances NUE by increasing nitrogen allocation and ammonium uptake under WST

The translational regulation of specific mRNAs implied that the translation of these transcripts is controlled independently of the overall translational state of the cell. The mechanisms underlying this type of regulation are not fully understood in most cases. However, it is believed to involve specific *trans* factors, including RNA-binding proteins, particular translation factors, ribosomal protein isoforms, small RNAs, and *cis*-regulatory elements within the target mRNAs (Merchante et al., 2017). To evaluate the role of the 5′ untranslated region (UTR) region in the three mRNAs (*AAP1*, *NPF7.3*, and *AMT1;1*) in rice, we generated transgenic rice plants overexpressing the FLAG- or GFP-tagged coding sequence (CDS) of these genes (Supplemental Figure 10A) and confirmed the presence of the transgenes using qRT–PCR analysis (Supplemental Figure 10B–10D). Following treatment with a TOR inhibitor or WST, we observed that the abundance of target proteins did not significantly decrease despite inhibition of TOR activity (Figure 5A–5C). This finding contrasted with the marked reduction in *de novo* synthesis of AAP1, NPF7.3, and AMT1;1

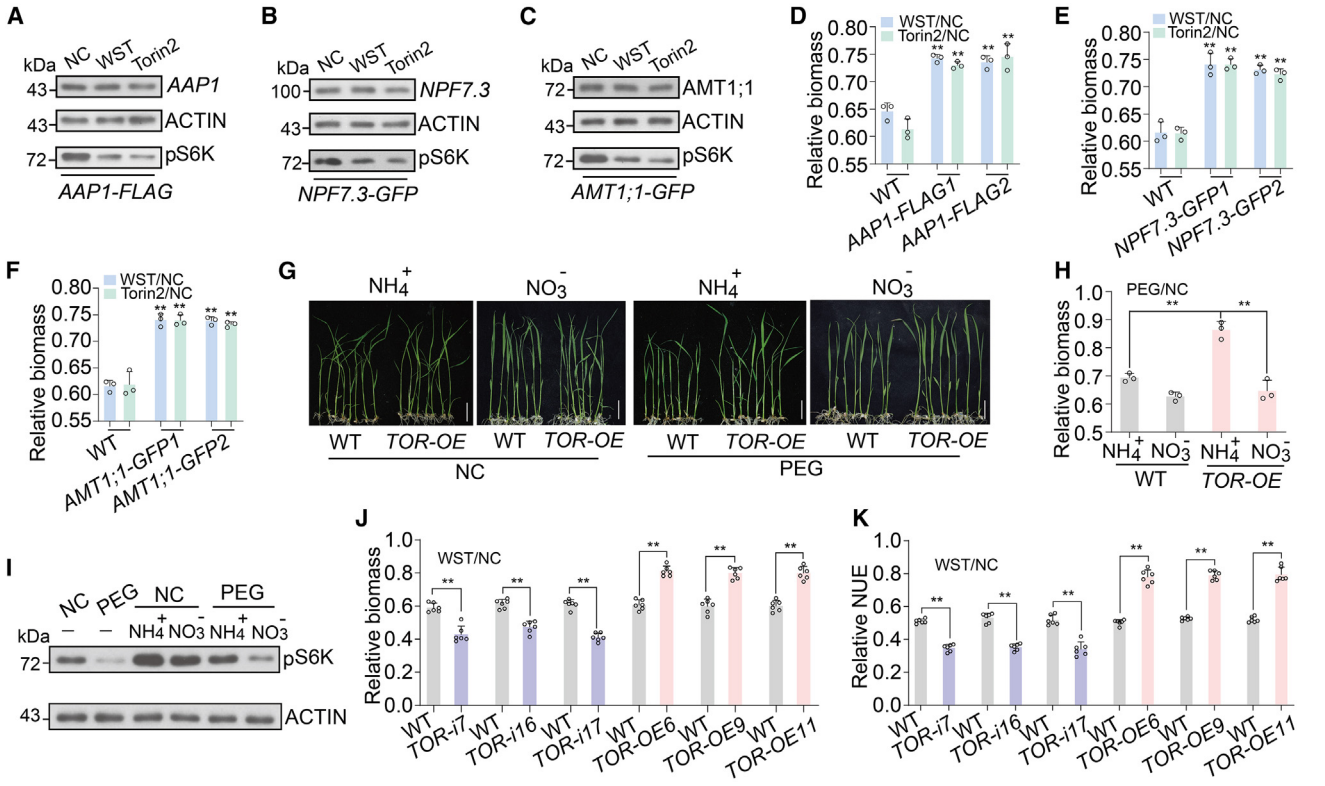

Figure 5. TOR enhances biomass and NUE by modulating *AAP1*, *NPF7.3*, and *AMT1;1*.

(A–C) TOR improves the accumulation of *AAP1* **(A)**, *NPF7.3* **(B)**, and *AMT1;1* **(C)** *in vivo* in stable transgenic lines at the seedling stage, as determined by immunoblot analyses. Torin2 treatment was performed at a concentration of 10 μM.

(D–F) Statistical data of relative above-ground biomass in transgenic lines *AAP1-FLAG* **(D)**, *NPF7.3-GFP* **(E)**, and *AMT1;1-GFP* **(F)** at 35 DAG after treatments with WST and Torin2. Error bars indicate means ± SD (n = 3). Statistical significance was assessed using two-tailed t-tests. $^{**}p < 0.01$.

(G and H) Performance and biomass investigation showed that PEG6000 (concentration at 8%) represses the activity of TOR activated by 50 mM nitrate (NO_3^-) or 50 mM ammonium (NH_4^+) in rice seedlings. Scale bar, 3 cm.

(I) Effects of NH_4^+ and NO_3^- on TOR activity in rice seedlings grown in medium with/without 8% PEG6000. Error bars indicate means ± SD (n = 3). Statistical significance was assessed using two-tailed t-tests. $^{**}p < 0.01$.

(J and K) Statistical data of above-ground biomass **(J)** and NUE **(K)** in *TOR* transgenic rice under NC and WST. Error bars indicate means ± SD (n = 6). Statistical significance was assessed using two-tailed t-tests. $^{**}p < 0.01$.

proteins observed in response to suppressed TOR activity (Figure 4) and the enhanced accumulation of protein in *TOR-OE* lines shown in Figure 4C, 4D, 4G, and 4H. These data suggested that TOR regulates the translation of the three mRNAs (*AAP1*, *NPF7.3*, and *AMT1;1*), potentially through the 5′ UTR regions absent in the CDS constructs in transgenic rice (Supplemental Figure 10A).

Previous studies have shown that the AAP subfamily members act as proton-coupled amino acid transporters for organic nitrogen uptake in plants (Fischer et al., 2002; Tegeder and Masclaux-Daubresse, 2018). On the other hand, rice PTR6 (NPF7.3) is responsible for transporting peptides across the vacuolar membrane for nitrogen allocation (Ouyang et al., 2010; Fang et al., 2017). Inorganic nitrogen uptake in rice is facilitated by ammonium transporters (AMTs) (Gazzarrini et al., 1999; Tegeder and Masclaux-Daubresse, 2018). Building upon published information and our aforementioned data confirming the translational regulation of the AAP1, NPF7.3, and AMT1;1 proteins by TOR signaling, we hypothesized that the translation of AAP1, NPF7.3, and AMT1;1 was involved in nitrogen uptake and allocation under WST. To test this hypothesis, we quantified nitrogen contents and observed that *AAP1* and *NPF7.3* RNA interference lines and *amt1;1* mutants displayed impaired abilities to assimilate nitrogen under WST (Supplemental Figure 10E–10I). Interestingly, rice overexpressing the CDSs of *AAP1*, *NPF7.3*, and *AMT1;1* demonstrated resistance to the decrease in translation associated with the suppression of TOR activity induced by WST or Torin2 treatment. This resistance resulted in the accumulation of relatively higher nitrogen levels in these plants (Supplemental Figure 10J–10L). Taking into consideration the enhanced nitrogen uptake and allocation, which can lead to increased biomass accumulation, we examined the relative biomass of rice seedlings after WST or Torin2 treatment. Strikingly, rice plants overexpressing the CDSs of *AAP1*, *NPF7.3*, and *AMT1;1* exhibited significantly higher relative biomass (Figure 5D–5F). Since TOR was unable to regulate the translation of those transcripts without a 5′ UTR sequence, nitrogen uptake and allocation were no longer repressed by WST. Thus, deregulation of the CDS for *AAP1*, *NPF7.3*, or *AMT1;1* could mitigate the growth retardation mediated by TOR signaling upon WST. Conversely, we observed that seedlings of the rice RNA interference lines *AAP1-i* and *NPF7.3-i* as well as *amt1;1* mutant seedlings produced relatively less biomass than the WT under

WST (Supplemental Figure 10M–10O). These findings suggested that WST restricts TOR-mediated nitrogen uptake and allocation in rice, partially through translational regulation.

Recent studies have shown that nitrogen plays a critical role as an upstream signal for TOR activation in animals and *Arabidopsis* (Cao et al., 2019; Kim and Guan, 2019; O'Leary et al., 2020; Liu et al., 2021). However, it remains unclear whether nitrogen-related nutrients regulate TOR signaling under WST. We examined the impact of different nitrogen sources, including NH_4^+, nitrate (NO_3^-), and glutamine on TOR activity in rice and found that these nitrogen sources effectively activated TOR activity (Supplemental Figure 10P). These findings aligned with previous studies in *Arabidopsis* (O'Leary et al., 2020; Liu et al., 2021; Ingargiola et al., 2023) demonstrating that nitrogen directly influences TOR activity.

Although different forms of nitrogen can efficiently activate the evolutionarily conserved TOR, plant species have distinct abilities to take up and utilize these nitrogen forms. In the case of rice, ammonium is generally considered the main nitrogen source (Wang et al., 1994; Cao et al., 2018; Guo et al., 2023). Previous studies have revealed that rice seedlings predominantly take up NH_4^+ in paddy fields and that rice supplied with NH_4^+ instead of NO_3^- exhibit better adaptation to drought stress (Yang et al., 2012; Ding et al., 2015; Cao et al., 2018). However, the underlying molecular mechanisms responsible for this preference remain unknown. To delve deeper into the roles of TOR in the differential uptake of NH_4^+ and NO_3^- under WST in rice, we devised a meticulously controlled approach. This involved simulating water-scarcity conditions using an 8% polyethylene glycol (PEG) solution while supplying the medium with NH_4^+ or NO_3^-. This method was established based on a previously published study (Cao et al., 2018) and ensured accurate simulation of water-saving conditions. Upon assessing biomass, we observed that *TOR-OE* rice displayed higher relative productivity when cultivated in a medium containing NH_4^+ as compared to one containing NO_3^-, under PEG treatment (Figure 5G and 5H). Subsequently, we investigated whether the two forms of inorganic nitrogen had distinct effects on TOR activity under PEG treatment. Utilizing immunoblot analyses to visualize TOR activity, we made an intriguing observation that TOR activity was effectively suppressed by 8% PEG6000, irrespective of the presence of sufficient inorganic nitrogen supplementation (Figure 5I). Significantly, NH_4^+ exhibited higher efficacy in mitigating the repression induced by water scarcity as compared to NO_3^- (Figure 5I). These findings shed light on the molecular mechanisms underlying rice's preference for NH_4^+ over NO_3^-, which involves translational regulation of mRNAs related to nitrogen uptake and allocation under WST.

To validate our hypothesis regarding the role of TOR in regulating rice production and NUE under WST, given that productivity during the reproductive period of a crop is one of the most important determinants of final crop yield, we conducted experiments focusing on the productivity of *TOR-i* and *TOR-OE* rice at the reproductive stage. As expected, we observed a notable positive correlation between relative biomass and NUE in relation to TOR expression levels following WST (Figure 5J and 5K; Supplemental Figure 10Q). These findings are consistent with our previous data showing that *TOR-OE* rice, which has higher TOR activity, exhibited higher relative levels of nitrogen, protein, and amino acids (Figure 1Q–1S).

DISCUSSION

In the pursuit of sustainable agriculture, there is an urgent need for advancements in crop germplasm innovation to develop resource-saving and environmentally friendly varieties (Yu et al., 2022; Hu et al., 2023). In many studies, the evaluation of stress-resistance genes has predominantly focused on assessing the survival rate under severe drought stress conditions (Waadt et al., 2022; Zhang et al., 2022a). However, there is still a lack of genes that have been proven to be highly effective in developing drought-resistant varieties. In contrast, WDR rice varieties have been successfully developed through conventional breeding of elite rice by harnessing genetic resources from ancient upland rice (Luo, 2010). Despite the potential benefits of developing water-saving rice varieties in terms of food security and mitigating global warming (Heredia et al., 2022; Xia et al., 2022), there are still fundamental scientific questions regarding the molecular mechanisms responsible for sustaining high productivity under WST.

We established an innovative water-saving strategy to assess the impact of WST on photosynthesis, water supply, and productivity in paddy-field rice (Figure 1A–1I). Our results demonstrated that WST represents an abiotic stressor that disrupts the equilibrium of energy absorption and redistribution in rice. Prior research has indicated that plant productivity is regulated by TOR-mediated networks, which coordinate nutrition and stress responses to sustain growth and energy redistribution. Additionally, the dynamics of nutrient acquisition are influenced by the dynamic nature of the environment (Baena-Gonzalez and Hanson, 2017; Li et al., 2021; Meng et al., 2022; Ye et al., 2022). In our previous study, we provided evidence that prolonged mild drought stress leads to a substantial decrease in the photosynthesis rate and impairs nutrient acquisition, resulting in reduced biomass and yield in rice (Du et al., 2018). In this study, we employed WST to simulate widely used water-saving strategies, commonly implemented in the cultivation of WDR rice varieties, for paddy-field rice (Figure 1A). Our in-depth analysis of polysome profiling data revealed that TOR-mediated translational repression occurs under WST, affecting mRNAs encoding proteins critical for nitrogen uptake and allocation, as well as components of the translation machinery such as proteins involved in the synthesis of tRNAs and ribosomes (Figure 1O–1P). Furthermore, our study provided additional evidence that *TOR-OE* rice have elevated levels of relative proteins, amino acids, and nitrogen (Figure 1Q–1S and Supplemental Table 2). Notably, these improvements in NUE were observed even under WST (Figure 5K). The relative proteins, amino acids, and nitrogen enhancements in TOR-OE rice were attributed to the upregulation of polysome loading and translation of mRNAs for proteins related to nitrogen uptake, underscoring the role of TOR regulation (Figures 4 and 5). Thus, TOR signaling emerged as a potential mechanism to enable rice plants to alleviate growth suppression caused by WST without significant negative consequences (Figure 6). A previous comprehensive proteomics analysis demonstrated that drought stress leads to a reduction in protein content in plants (Heinemann et al., 2021). Likewise, we observed similar alterations in rice following

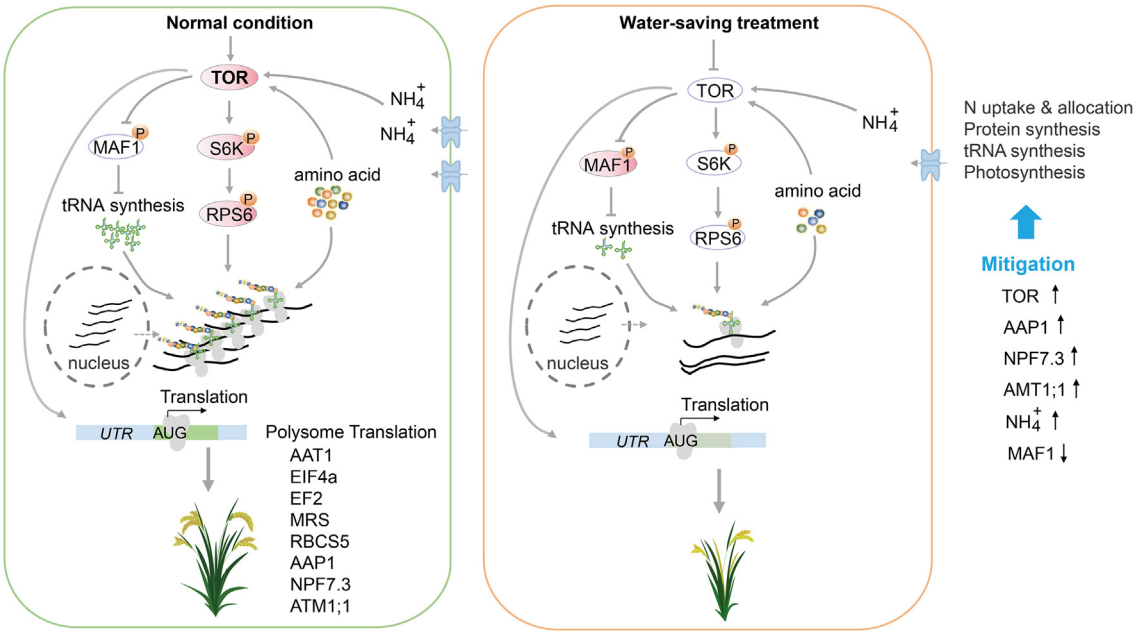

Figure 6. A proposed model illustrating how TOR signaling modulates rice growth under normal or water-saving treatment.
Under normal conditions, the TOR-S6K-RPS6 module and the TOR-MAF1 module work together to regulate protein translation and the biosynthesis of pre-tRNA in rice cells. This coordinated regulation allows optimal protein synthesis. Additionally, TOR can regulate protein synthesis by controlling the UTR regions of specific nitrogen assimilation-related genes such as *AAP1*, *NPF7.3*, and *AMT1;1*. This regulation ensures normal NH_4^+ absorption and utilization in rice, which in turn promotes TOR activity and supports the normal growth of rice. However, under water-saving treatment (WST), TOR activity is inhibited. This inhibition leads to the phosphorylation of MAF1 and the inhibition of S6K-RPS6 signaling. As a result, tRNA biogenesis and protein translation efficiency are affected. Furthermore, the translation of AAP1, NPF7.3, and AMT1;1 is suppressed, leading to reduced NH_4^+ absorption and nitrogen allocation efficiency, thereby reducing nitrogen use efficiency (NUE) and protein synthesis, ultimately causing growth retardation and reduced biomass in rice under WST. In TOR-OE rice, TOR remains more active when exposed to WST, which helps to maintain a certain level of inhibition of the phosphorylation of MAF1. Additionally, the inhibition of S6K-RPS6 signaling and translational inhibition of AAP1, NPF7.3, and AMT1;1 are also greatly reduced. This leads to significant improvements in tRNA biogenesis, protein translation efficiency, and NH_4^+ uptake and nitrogen allocation efficiency in TOR-OE rice under WST. The ability of TOR-OE rice to grow under WST is evident in the model, where pink modules represent higher levels of expression or phosphorylation and light modules indicate lower levels.

WST, which could be attributed to TOR-mediated adaptation to water deficit. This adaptation was likely responsible for the down-regulation of energy-consuming processes and the consequent growth inhibition. Furthermore, the decline in nitrogen-derived amino acid pools may fine-tune TOR activity through instant feedback, as amino acids act as upstream signals for TOR activation (Figure 6 and Supplemental Figure 10P) (Cao et al., 2019; O'Leary et al., 2020; Liu et al., 2021). Thus, TOR signaling under WST represents a novel adaptation mechanism that maintains cellular energy homeostasis under conditions of limited nitrogen availability through the integration of nitrogen capture and protein translation (Figure 6).

The translation machinery, which includes tRNAs, ribosomes, and translation regulators, plays crucial roles in translational control. Translational regulators transmit growth, development, and stress signals to the translation machinery (Merchante et al., 2017), where global or selective translational control occurs to modulate mRNA translation efficiency. Under severe stresses such as salinity, water deficit, and extreme temperatures, the energetically demanding translation machinery is slowed down, resulting in a significant decrease in global translation rates (Kawaguchi et al., 2003; Matsuura et al., 2013; Merret et al., 2015; Wang et al., 2017). Despite the identification of translational repression under various stress conditions, the underlying biological mechanisms responsible for this phenomenon remain largely unknown.

Activation of TOR promotes overall translation by stimulating ribosome biogenesis, assembly, and initiation of translation, leading to increased global protein synthesis (Lee et al., 2017; Chen et al., 2018; Schepetilnikov and Ryabova, 2018; Ahn et al., 2019; Scarpin et al., 2020, 2022; Dong et al., 2023). However, the specific role of TOR signaling in alleviating abiotic stress in plants remains largely unexplored. By performing molecular, biochemical, and genetic analyses, we uncovered the participation of RPS6a/eS6 as a downstream target of TOR-S6K signaling under WST (Figure 2A–2C). The ribosome-loading efficiency data obtained from *rps6a* mutants provided additional evidence supporting the participation of the TOR-S6K-RPS6a module in the global repression of translation under WST (Figure 2I and Supplemental Figure 6F). These findings highlighted the crucial role of RPS6a in regulating ribosome-loading efficiency during the adaptation mediated by TOR signaling under WST. Furthermore, we observed that rice *maf1* mutants displayed enhanced productivity, accompanied by increased relative tRNA and total protein accumulation (Figure 3). Subsequent biochemical and genetic assays confirmed that TOR-MAF1-mediated Pol III activity also contribute to the reduction in tRNA biosynthesis under WST (Figure 3D–3F).

Consequently, the availability of tRNAs for translation is reduced, leading to global translational repression under WST. In summary, our findings offer direct evidence of a decrease in translation capacity in rice as a result of WST. This reduction can be partially attributed to the TOR-S6K-RPS6a and TOR-MAF1 modules (Figure 6). Nevertheless, the precise components of the dynamic translation machinery governed by TOR signaling under WST at the biochemical and genetic levels have yet to be fully elucidated. Further integrated studies are required to unravel the intricate mechanisms underlying TOR signaling under stress conditions.

Notably, published data have highlighted the involvement of nitrogen assimilation in drought stress, with ABI2 (ABA insensitive 2), a phosphatase inhibited by ABA, identified as a key positive regulator of the nitrate transporter NPF6.3 (Leran et al., 2015). Additionally, key enzymes involved in nitrogen allocation or remobilization processes, such as OsGS1;1 and OsNADH-GOGAT2, have been shown to play important roles in plant productivity under abiotic stress. For instance, co-overexpression of *OsGS1;1* and *OsGS2* leads to increased yield under drought and salinity stress in rice (James et al., 2018), indicating the significance of nitrogen allocation in enhancing plant productivity under adverse conditions. Recently, the DST-NR1.2 signaling pathway was discovered to control rice NUE by affecting nitrogen assimilation under drought stress (Han et al., 2022). However, the coupling of drought tolerance and nitrogen assimilation mediated by DST limits its application in engineering drought-tolerant rice varieties with higher NUE.

In our study, we discovered that rice TOR plays a crucial role in maintaining significant relative biomass and NUE under WST by stabilizing the translation machinery and improving nitrogen uptake and allocation. To elucidate the underlying mechanism, we conducted *in vivo* and *in vitro* assays, which revealed that AAP1, NPF7.3, and AMT1;1 are subjected to translational regulation by TOR signaling (Figures 4 and 5A–5C). Moreover, our data also demonstrated the crucial role of the 5′ UTR region in *AAP1*, *NPF7.3*, and *AMT1;1* in the potential specific translational control mediated by TOR. Importantly, the constitutive overexpression of the CDSs of *AAP1*, *NPF7.3*, and *AMT1;1* resulted in the maintenance of high relative nitrogen content and an increase in relative biomass production under WST (Figure 5D–5F and Supplemental Figure 10J–10L). These novel findings suggested that TOR signaling could alleviate growth retardation and enhance nitrogen accumulation under WST, potentially through both global and specific translational regulation mechanisms (Figure 6). However, further studies are required to elucidate the biological basis of how TOR regulates the translation of specific genes.

Ammonium has been recognized as the primary nitrogen source for paddy-field rice (Wang et al., 1993). In the rhizosphere, where oxygen is transported by aerenchyma cells in the roots, nitrate can be converted to ammonium through the nitrogen assimilation pathway (Li et al., 2008; Nojiri et al., 2020). Previous studies found that the uptake of ammonium in rice is significantly reduced under drought conditions (Foyer et al., 1998; Xu and Zhou, 2006). Despite the importance of ammonium for rice, the molecular mechanisms underlying the repression of ammonium absorption remain unknown. Here, we presented biochemical and genetic evidence indicating that TOR signaling regulates the translation of an ammonium transporter, known as AMT1;1, under WST in rice (Figure 4). Through further genetic and physiological analyses, we discovered that rice AMT1;1 is under translational control by TOR signaling. Moreover, we found that *amt1;1* mutants exhibited a considerable decrease in both nitrogen accumulation and biomass under WST (Supplemental Figure 10I and 10O). These findings provided compelling evidence that the repression of ammonium uptake during WST is primarily due to the decreased translation of *AMT1;1*, which is related to the inhibition of TOR activity. Additionally, *TOR-OE* rice can effectively balance productivity and defense tradeoffs by improving the translation of AMT1s. In *Arabidopsis*, various nitrogen signals have been shown to activate TOR signaling directly (Cao et al., 2019; O'Leary et al., 2020; Liu et al., 2021; Ingargiola et al., 2023). In this study, we found that nitrate, ammonium, and glutamine could efficiently activate TOR in rice (Supplemental Figure 10P). However, when we used an 8% PEG treatment to mimic WST, we surprisingly found that ammonium stimulated TOR activity more strongly than nitrate (Figure 5I). This finding suggested that there is a hierarchy in the nitrogen sources promoting TOR activation, with ammonium being more effective than nitrate in rice. Furthermore, we demonstrated that *TOR-OE* rice exhibited higher relative biomass when fed with ammonium rather than nitrate (Figure 5G and 5H). Taken together, our data indicated that ammonium is crucial for activating TOR and promoting the translation machinery, thereby enhancing nitrogen uptake and allocation in rice under WST (Figure 6).

In summary, our findings collectively demonstrated that the TOR signaling pathway plays a crucial role in mediating the biosynthesis of tRNA and enhancing translation efficiency, thereby regulating the translational machinery responsible for protein synthesis under WST. Additionally, TOR promotes the translation of specific genes involved in NH_4^+ absorption and nitrogen allocation to improve nutrient uptake and utilization (Figure 6). Thus, TOR plays a pivotal role in mediating the translation of genes related to nitrogen uptake and allocation, thereby regulating both productivity and NUE under WST. This discovery of the TOR regulatory system offers valuable insights for the development of novel breeding strategies that involve overexpressing TOR to mitigate the tradeoff between grain yield and water conservation in crop production (Figure 6). Therefore, our study presents a promising strategy to balance crop yields and water conservation by moderately enhancing TOR signaling without incurring severe yield penalties, facilitating the development of low-carbon agriculture worldwide.

METHODS

Vector construction and rice transformation

The *maf1* and *rps6a* mutants were created using the CRISPR-Cas9 system in the *Kitaake* background (*Oryza sativa* L. ssp. *japonica*). The CRISPR-Cas9 plasmids were constructed, and guide sequences of 20 base pairs were selected and analyzed for targeting specificity using CRISPR-P 2.0 (Liu et al., 2017). Genomic DNA was extracted from the transgenic lines using the cetyltrimethylammonium bromide method. The genomic regions surrounding the CRISPR target sites were amplified by PCR with specific primers (Supplemental Table 1), and the resulting segments were subjected to Sanger sequencing to identify mutations.

For the overexpression of rice *S6K1* and *TOR* in the *Kitaake* background, the sequences encoding fusion proteins, *S6K1-FLAG* and *TOR-FLAG*,

were cloned into a binary vector (pCAMBIA1300) under the control of the *Zea mays UBIQUITIN* (*UBI*) gene promoter, utilizing the Monclone kit (Monad Biotech, China). The plasmids were transformed into *Agrobacterium* strain EHA105, and rice transformation was performed as previously described (Hiei et al., 1994). Transgenic plants were identified using specific primers (Supplemental Table 1). The *TOR-i* rice was generated using a 312-bp fragment specific to the *TOR* gene (Os05g0235300) as the targeting site in the RNAi backbone vector pTCK303. All plants used for propagation were grown in paddy fields in Hainan during the winter and in Hangzhou during the summer.

The rice *AAP1* and *NPF7.3* overexpression lines and RNA interference lines were in the *ZhongHua11* background (*O. sativa* L. ssp. *japonica*), as produced in previous studies (Fang et al., 2017; Ji et al., 2020). The *amt1;1* knockout mutants were generated using the CRISPR-Cas9 tool in the rice cultivar *Nipponbare* (*O. sativa* L. ssp. *japonica*), as described previously (Li et al., 2016).

Treatments and physiological measurements

For the WST throughout the life cycle, seeds of T_1 or T_2 overexpression lines and mutants were germinated on Murashige and Skoog (MS) medium supplemented with 50 mg/l hygromycin for selection. Five days after germination (DAG), the seedlings were transferred to a 17-l bucket, with two plants of each line occupying half of the bucket. To maintain the desired SWC, the SWC was regularly monitored using a TRIME-PICO TDR device. Water was added as needed to maintain the SWC within the target range of 25%–30% from 20 DAG to 50 DAG, 30%–40% from 5 DAG to 20 DAG, and 30%–40% from 50 DAG to 80 DAG. During the seedling stage, WST was implemented by maintaining the SWC within the range of 25%–30% from 28 DAG to 35 DAG. At 35 DAG, photographs were taken or sampling was conducted, depending on the specific experimental requirements.

For the treatment with TOR inhibitors Torin2 (Macklin, 1 223 001-51-1) and AZD8055 (Macklin, 1 009 298-09-2), we followed a previously published method with slight modifications (Sun et al., 2016). In brief, the inhibitors were dissolved in dimethyl sulfoxide (DMSO) to prepare 10 mM stock solutions. These stock solutions were then aliquoted and stored at −20°C for future use. Prior to usage, the working concentration of 10 μM was prepared by diluting the stock solution for spreading on rice seedlings. Specifically, 1 ml of the working solution was applied to each seedling at 28 DAG, with subsequent applications every 2 days for a total duration of 7 days before sampling for physiological assays. The TOR inhibitor treatments to protoplasts were carried out after transfection, using a final concentration of 10 μM in W5 solution. As controls for the TOR inhibitor treatment, we used a working concentration of an equal volume of DMSO at 0.01 μM. The controls were subjected to the same treatment procedure as described above. The photosynthetic rate was measured on the youngest fully developed leaves at 35 DAG using a portable photosynthesis system (LI-6400; Li-Cor, Lincoln, NE, USA) equipped with a red-/blue-light-emitting diode light source (6400-02B; Li-Cor). Pollen viability was analyzed by incubating mature anthers with 1% (w/v) I_2-KI staining solution. Images were captured and recorded using a Leica DMIRB fluorescence microscope.

Seedling treatment with ammonium and nitrate

T_2 seeds of transgenic rice lines and WT were sterilized and germinated in MS medium. After 5 days, seedlings of similar size were transferred to sterile glass tubes containing a nutrient solution composed of 0.5 mM $MgSO_4 \cdot 7H_2O$, 0.4 mM $CaCl_2$, 0.2 mM KCl, 0.2 mM $NaH_2PO_4 \cdot 2H_2O$, 0.1 mM NH_4NO_3, 10 μM $MnCl_2 \cdot 4H_2O$, 30 μM $FeSO_4 \cdot 7H_2O$-EDTA, 10 μM H_3BO_3, 0.5 μM $ZnSO_4 \cdot 7H_2O$, 0.2 μM $CuSO_4$, 0.1 μM $Na_2MoO_4 \cdot 4H_2O$, and 7 g/l plant agar. The pH of the solution was adjusted to 5.5 using a 5 mM 4-morpholineethanesulfonic acid (MES) buffer. The following treatments were applied in the nutrient solution: 1 mM NH_4^+, 1 mM NO_3^-, 1 mM NH_4^+ with 8% PEG6000, and 1 mM NO_3^- with 8% PEG6000. These treatments were maintained for 10 days before samples were harvested. The experiments were conducted in a growth chamber with a photoperiod of 14 h light and 10 h darkness, a light intensity of 500 μmol m^{-2} s^{-1}, relative humidity of approximately 60%, and temperatures of 30°C and 25°C during the day and night, respectively.

Total protein, nitrogen, amino acids, and nitrogen use efficiency

For the total protein assay, 10 mg of lyophilized plant powder was dissolved in 700 μl of methanol and incubated at 65°C for 30 min. The resulting pellets were washed twice with 1 ml of 70% ethanol (v/v) after centrifugation (15 min, 4°C, 16 000 *g*) and then resuspended in 500 μl of 0.1 M NaOH. The solution was further incubated at 95°C in a shaking water bath for 1 h before centrifugation. The protein content of the supernatant was quantified using Coomassie brilliant blue G250 Assay Reagent (Vazyme, China). To measure the total nitrogen content in rice, a TOC/TN analyzer (Shimadzu, Japan) equipped with TNM-1 attachments was used following a previously established method (Hoosbeek et al., 2006). For the measurement of total amino acids, the high-performance liquid chromatography (HPLC) method was employed as described in previous studies (Sanders et al., 2009). Single free amino acids were extracted and measured using HPLC with an amino acid analyzer (Hitachi, Japan), following a detailed method outlined in Ji et al. (2020). NUE was determined by taking the ratio of total grain yield to applied N fertilizer.

Isolation of total RNA, polysomal RNA, and non-polysomal RNA

Total RNA was extracted from rice tissues using RNA isolater Total RNA Extraction Reagent (Vazyme, China). The quality and quantity of the extracted RNA were assessed using a NanoDrop 1000 spectrophotometer (Thermo Fisher Scientific, USA). For polysome profiling analyses, we followed a previously described method (Kawaguchi et al., 2003) with slight modifications. Rice leaves were harvested and ground in liquid nitrogen. To separate P and NP RNAs, 1.0 ml of frozen seedling powder was mixed with 1.0 ml of polysome extraction buffer (200 mM Tris–HCl [pH 8.5], 25 mM $MgCl_2$, 50 mM KCl, 50 μg/ml cycloheximide, 100 μg/ml heparin, 400 U/ml RNAsin, 2% polyoxyethylene 10 tridecyl ether, 1% deoxycholic acid, and 1% [v/v] NP-40). After incubation on ice for 5 min with gentle inversion, cell debris was removed by centrifugation at 12 000 *g* for 5 min at 4°C. Next, 750 μl of plant extract was carefully layered on top of a 15%–50% sucrose gradient in a 12-ml tube. The tubes were then centrifuged at 210 000 *g* using a Beckman ultracentrifuge at 4°C for 3.5 h. This resulted in the distribution of P RNAs within the sucrose gradient based on their sedimentation coefficient. Fourteen fractions were collected using a density gradient fractionator (ISCO, Lincoln, NE, USA), including NP and P fractions. The P fractions were further divided into mixed fractions 1–7 and mixed fractions 8–14. Total RNA from the P or NP fractions was then extracted using acid-phenol-chloroform (pH 4.5), followed by lithium chloride precipitation. The RNA quantified using a Qubit 3.0 (Thermo Fisher) was dissolved in diethyl pyrocarbonate-treated ultrapure H_2O for subsequent RNA-seq at Novogene Bioinformatics Technology or qPCR assays performed using MQ00801-MonAmp Universal ChemoHS Specificity Plus qPCR Mix (Monad Biotech, China). The *ACTIN* gene was used as an internal control to normalize the expression levels of target genes. The percentage of P RNA relative to total RNA (NP + P) was calculated using the formula: RNA in polysomes % = (amount of PRNA/amount of P and NP RNA) × 100%.

RNA-seq analyses

The mRNA was extracted from the total RNA, specifically from the P or NP fractions, using the mRNA Isolation Master Kit (Yeasen, China). The extracted mRNA was then used to construct sequencing libraries with the TruSeq PE Cluster Kit v3-cBot-HS (Illumina). These libraries were subjected to high-throughput sequencing on a HiSeq-PE150 (Illumina) platform at Novogene Bioinformatics Technology (China). To ensure data quality, raw sequencing reads were filtered by Trimmomatic (version 0.39). The filtered reads were then aligned to the rice genome (MSU RGAP, release 7) using HISAT2 (version 2.0.5) with default parameters. The abundance of annotated reference genes was quantified utilizing StringTie (version 2.0). Differential expression analysis was performed using DESeq2, considering genes

with a multiple-test corrected *p* value of less than 0.05 as differentially expressed. To assess the effects of WST on P mRNA, hierarchical clustering analysis was conducted using the ratio of WST-treated P mRNA to (P mRNA+NP) mRNA and the ratio of P mRNA to (P mRNA+NP mRNA) under normal conditions.

Co-immunoprecipitation assay

To study the interaction between TOR and S6K1 in rice, we isolated protoplasts from the leaves of 15-day-old seedlings. The fusion proteins TOR-HA and S6K1-FLAG were co-expressed in protoplasts for 12 h. The total protein from the protoplasts was extracted using a lysis buffer consisting of 50 mM Tris–HCl (pH 7.5), 150 mM NaCl, 5 mM EDTA, 1 mM dithiothreitol (DTT), 1% Triton X-100, and 1× protease inhibitor cocktail (Complete Mini, Roche, USA). The protein extracts were then incubated with 1 μg of HA antibody (Sigma, USA) at 4°C for 3 h, followed by an additional 3-h incubation with protein G Sepharose beads (GE Healthcare, USA). The immunoprecipitated protein on the beads was washed three times with lysis buffer. Subsequently, the proteins were eluted from the beads by adding 20 μl of 2× SDS loading buffer. After separation on a 10% SDS–PAGE gel, the presence of TOR-HA in the input sample was detected using an anti-HA antibody. Anti-FLAG antibody was used to detect S6K1-FLAG from the beads before and after immunoprecipitation.

In vitro kinase assay

For *in vitro* kinase assays, TOR-HA and S6K1-HA kinase fusions were separately expressed in rice protoplasts and purified from 4×10^5 protoplasts as follows. Protoplasts were lysed in 1 ml of immunoprecipitation buffer containing 50 mM Tris–HCl (pH 7.5), 150 mM NaCl, 5 mM EDTA, 1 mM DTT, 2 mM NaF, 2 mM Na_3VO_4, 1% Triton X-100, and 1× protease inhibitor cocktail (Complete Mini, Roche). The protein extracts were incubated with 2 μg of anti-HA antibody (Sigma, H9658) at 4°C for 2 h and an additional 1 h with protein G Sepharose beads (GE Healthcare). The immunoprecipitated kinase protein was washed three times with immunoprecipitation buffer and once with kinase buffer for S6K1 (25 mM Tris–HCl [pH 8.0], 100 mM NaCl, 10 mM $MgCl_2$, 5 mM $CaCl_2$, and 1 mM DTT) and kinase buffer for TOR (25 mM HEPES [pH 7.4], 50 mM KCl, 10 mM $MgCl_2$, 10 μM cold ATP). The substrates rice Maf1-His and RPS6a-His were expressed in *E. coli* strain BL21 cells and purified. *In vitro* kinase assays were performed by incubating purified kinase and 0.2 μg of substrate in a reaction buffer containing 25 mM Tris–HCl (pH 8.0), 100 mM NaCl, 10 mM $MgCl_2$, 5 mM $CaCl_2$, 0.1 μM ATP, and 6 μCi [γ-^{32}P]ATP at 30°C for 30 min for the S6K1-RPS6a kinase assay. For the TOR-Maf1 kinase assay, reactions were performed in 25 mM HEPES (pH 7.4), 50 mM KCl, 10 mM $MgCl_2$, 0.1 μM ATP, and 6 μCi [γ-^{32}P]ATP at 30°C for 30 min. The reaction was stopped by adding 15 μl of 6× SDS–PAGE loading buffer. After the separation of the proteins on a 15% SDS–PAGE gel, protein kinase activity was detected on the dried gel using a Typhoon imaging system (GE Healthcare).

Analyses of *de novo* protein synthesis

To analyze *de novo* protein synthesis, we constructed vectors expressing the HA-tag fused to the genomic sequence of *AAP1* (Os07g0134000), *NPF7.3* (Os04g0597800), *AMT1;1* (Os04g0509600), or *ACTIN* (Os03g0718100). Each vector (100 μg) was expressed in rice protoplasts. The protoplasts (5×10^6) were divided into three groups for different treatments: 0.01 μM DMSO, 10 μM Torin2, or 10 μM AZD8055. After incubation in W5 solution (containing 2 mM MES [pH 5.7], 154 mM NaCl, 125 mM $CaCl_2$, and 5 mM KCl) for 6 h, the protoplasts were harvested for western blot analysis and qRT–PCR assays using kits from Monad Biotech, China. For qRT–PCR, forward and reverse primers were designed to cover the fusion connector of the 3′ HA tag and 5′ HA tag. The specific primer sequences are provided in Supplemental Table 1.

Antibodies and western blot analyses

Commercial phosphorylated S6K1 polyclonal rabbit antibody (Agrisera, AS132664) and phosphorylated RPS6 polyclonal rabbit antibody (Agrisera, AS194291) were used to detect phosphorylation of S6K1 and RPS6 in rice, respectively. Commercial anti-AMT1;1 rabbit polyclonal antibody (PhytoAB, PHY0962S) and anti-ACTIN rabbit polyclonal antibody (Sangon Biotech, D110007-0100) were used to detect AMT1;1 and ACTIN in rice, respectively. Mouse monoclonal anti-FLAG M2 (Sigma, F1804), anti-HA antibody (Sigma, H9658), and anti-GFP from rabbit (Sigma, AB10145) were used to detect tagged fused proteins. Quantification of the band intensities in the protein blot were performed using Image Lab (Bio-Rad). The relative value of each band represents the ratio of band intensity to the band intensity of the loading control.

DATA AVAILABILITY

Sequencing data have been deposited in the Chinese National Genome Data Center under accession number CRA013631.

SUPPLEMENTAL INFORMATION

Supplemental information is available at *Molecular Plant Online*.

FUNDING

We thank Prof. Guohua Xu (College of Resources and Environmental Sciences, Nanjing Agricultural University, Nanjing, China) and Dr. Chang Li (College of Resources and Environmental Sciences, Henan Agricultural University, Zhengzhou, China) for proving rice *amt1;1* mutants. We thank Prof. Bin Hu (Guangdong Laboratory for Lingnan Modern Agriculture, State Key Laboratory for Conservation and Utilization of Subtropical Agro-Bioresources, College of Agriculture, South China Agricultural University, Guangzhou, 510 642, China) for proving rice *AMT1;1-GFP* lines. We thank Siyuan Sun and Qiye Ni (College of Agriculture and Biotechnology, Zhejiang University, Hangzhou, China) for managing transgenic rice. Prof. Lizhong Xiong (National Key Laboratory of Crop Genetic Improvement and National Center of Plant Gene Research, Hubei Hongshan Laboratory, Huazhong Agricultural University, Wuhan, 430 070, China) for critical discussion and editing of the manuscript. Thise research was supported by the Hainan Provincial Joint Project of Sanya Yazhou Bay Science and Technology City City (320LH031 and HSPHDSRF-2023-04-016), Zhejiang Provincial Natural Science Foundation of China (LY21C020003), Zhejiang University Global Partnership Fund, Fundamental Research Funds for the Central Universities for the Central Universities (K20200168), the Key Research and Development Program of Zhejiang (2020C02002), National Natural Science Foundation of China (32201819), and China Postdoctoral Science Foundation (2022M712807). J.S. is supported by the NIH grant GM129093.

AUTHOR CONTRIBUTIONS

H.D. and W.L. initiated the project and H.D., W.L., and J.S. wrote and finalized the manuscript. H.D., W.L., J.L., Z.L., R.Y., W.C., Y.H., Y.Y., Y.Z., H.H., and P.Z., designed and performed most of the experiments. J.S., R.Y., Z.F., Z.T., S.S., R.P., J.Z., and J.T. provided assistance and suggestions. All authors discussed the results and commented on the manuscript.

ACKNOWLEDGMENTS

We thank Prof. Guohua Xu (College of Resources and Environmental Sciences, Nanjing Agricultural University, Nanjing, China) and Dr. Chang Li (College of Resources and Environmental Sciences, Henan Agricultural University, Zhengzhou, China) for providing rice *amt1;1* mutants. We thank Prof. Bin Hu (Guangdong Laboratory for Lingnan Modern Agriculture, State Key Laboratory for Conservation and Utilization of Subtropical Agro-Bioresources, College of Agriculture, South China Agricultural University, Guangzhou, China) for providing rice *AMT1;1-GFP* lines. We thank Siyuan

Sun and Qiye Ni (College of Agriculture and Biotechnology, Zhejiang University, Hangzhou, China) for managing transgenic rice, and Prof. Lizhong Xiong (National Key Laboratory of Crop Genetic Improvement and National Center of Plant Gene Research, Hubei Hongshan Laboratory, Huazhong Agricultural University, Wuhan, China) for critical discussion and editing of the manuscript. The authors declare no competing interests.

Received: September 18, 2023
Revised: November 29, 2023
Accepted: December 1, 2023
Published: December 5, 2023

REFERENCES

Ahn, C.S., Lee, D.H., and Pai, H.S. (2019). Characterization of Maf1 in *Arabidopsis*: function under stress conditions and regulation by the TOR signaling pathway. Planta **249**:527–542.

Baena-González, E., and Hanson, J. (2017). Shaping plant development through the SnRK1-TOR metabolic regulators. Curr. Opin. Plant Biol. **35**:152–157.

Bakshi, A., Moin, M., Gayatri, M.B., Reddy, A.B.M., Datla, R., Madhav, M.S., and Kirti, P.B. (2023). Involvement of Target of Rapamycin (TOR) Signaling in the Regulation of Crosstalk between Ribosomal Protein Small Subunit 6 Kinase-1 (RPS6K-1) and Ribosomal Proteins. Plants **12**:176.

Blayney, J., Geary, J., Chrisp, R., Violet, J., Barratt, L., Tavukçu, L., Paine, K., Vaistij, F.E., Graham, I.A., Denby, K.J., and White, R.J. (2022). Impact on *Arabidopsis* growth and stress resistance of depleting the Maf1 repressor of RNA polymerase III. Gene **815**, 146130.

Cao, P., Kim, S.J., Xing, A., Schenck, C.A., Liu, L., Jiang, N., Wang, J., Last, R.L., and Brandizzi, F. (2019). Homeostasis of branched-chain amino acids is critical for the activity of TOR signaling in *Arabidopsis*. Elife **8**, e50747.

Cao, X., Zhong, C., Zhu, C., Zhu, L., Zhang, J., Wu, L., and Jin, Q. (2018). Ammonium uptake and metabolism alleviate PEG-induced water stress in rice seedlings. Plant Physiol. Biochem. **132**:128–137.

Chen, G.H., Liu, M.J., Xiong, Y., Sheen, J., and Wu, S.H. (2018). TOR and RPS6 transmit light signals to enhance protein translation in deetiolating *Arabidopsis* seedlings. Proc. Natl. Acad. Sci. USA **115**:12823–12828.

Chiocchetti, A., Zhou, J., Zhu, H., Karl, T., Haubenreisser, O., Rinnerthaler, M., Heeren, G., Oender, K., Bauer, J., Hintner, H., et al. (2007). Ribosomal proteins Rpl10 and Rps6 are potent regulators of yeast replicative life span. Exp. Gerontol. **42**:275–286.

Cramer, M.D., Hoffmann, V., and Verboom, G.A. (2008). Nutrient availability moderates transpiration in Ehrharta calycina. New Phytol. **179**:1048–1057.

Creff, A., Sormani, R., and Desnos, T. (2010). The two *Arabidopsis RPS6* genes, encoding for cytoplasmic ribosomal proteins S6, are functionally equivalent. Plant Mol. Biol. **73**:533–546.

Ding, L., Gao, C., Li, Y., Li, Y., Zhu, Y., Xu, G., Shen, Q., Kaldenhoff, R., Kai, L., and Guo, S. (2015). The enhanced drought tolerance of rice plants under ammonium is related to aquaporin (AQP). Plant Sci. **234**:14–21.

Dong, Y., Srour, O., Lukhovitskaya, N., Makarian, J., Baumberger, N., Galzitskaya, O., Elser, D., Schepetilnikov, M., and Ryabova, L.A. (2023). Functional analogs of mammalian 4E-BPs reveal a role for TOR in global plant translation. Cell Rep. **42**:112892.

Du, H., Chang, Y., Huang, F., and Xiong, L. (2015). GID1 modulates stomatal response and submergence tolerance involving abscisic acid and gibberellic acid signaling in rice. J. Integr. Plant Biol. **57**:954–968.

Du, H., Wang, N., Cui, F., Li, X., Xiao, J., and Xiong, L. (2010). Characterization of the beta-carotene hydroxylase gene *DSM2* conferring drought and oxidative stress resistance by increasing xanthophylls and abscisic acid synthesis in rice. Plant Physiol. **154**:1304–1318.

Du, H., Huang, F., Wu, N., Li, X., Hu, H., and Xiong, L. (2018). Integrative Regulation of Drought Escape through ABA-Dependent and -Independent Pathways in Rice. Mol. Plant **11**:584–597.

Fan, X., Xie, D., Chen, J., Lu, H., Xu, Y., Ma, C., and Xu, G. (2014). Overexpression of *OsPTR6* in rice increased plant growth at different nitrogen supplies but decreased nitrogen use efficiency at high ammonium supply. Plant Sci. **227**:1–11.

Fang, Z., Bai, G., Huang, W., Wang, Z., Wang, X., and Zhang, M. (2017). The Rice Peptide Transporter OsNPF7.3 Is Induced by Organic Nitrogen, and Contributes to Nitrogen Allocation and Grain Yield. Front. Plant Sci. **8**:1338.

Fischer, W.N., Loo, D.D.F., Koch, W., Ludewig, U., Boorer, K.J., Tegeder, M., Rentsch, D., Wright, E.M., and Frommer, W.B. (2002). Low and high affinity amino acid H^+-cotransporters for cellular import of neutral and charged amino acids. Plant J. **29**:717–731.

Flexas, J., Bota, J., Galmés, J., Medrano, H., and Ribas-Carbó, M. (2006). Keeping a positive carbon balance under adverse conditions: responses of photosynthesis and respiration to water stress. Physiol. Plantarum **127**:343–352.

Foyer, C.H., Valadier, M.H., Migge, A., and Becker, T.W. (1998). Drought-induced effects on nitrate reductase activity and mRNA and on the coordination of nitrogen and carbon metabolism in maize leaves. Plant Physiol. **117**:283–292.

Gazzarrini, S., Lejay, L., Gojon, A., Ninnemann, O., Frommer, W.B., and von Wirén, N. (1999). Three functional transporters for constitutive, diurnally regulated, and starvation-induced uptake of ammonium into *Arabidopsis* roots. Plant Cell **11**:937–948.

Guo, X., Chen, Y., Hu, Y., Feng, F., Zhu, X., Sun, H., Li, J., Zhao, Q., and Sun, H. (2023). OsMADS5 interacts with OsSPL14/17 to inhibit rice root elongation by restricting cell proliferation of root meristem under ammonium supply. Plant J. **116**:87–99.

Gururani, M.A., Venkatesh, J., and Tran, L.S.P. (2015). Regulation of Photosynthesis during Abiotic Stress-Induced Photoinhibition. Mol. Plant **8**:1304–1320.

Han, M.L., Lv, Q.Y., Zhang, J., Wang, T., Zhang, C.X., Tan, R.J., Wang, Y.L., Zhong, L.Y., Gao, Y.Q., Chao, Z.F., et al. (2022). Decreasing nitrogen assimilation under drought stress by suppressing DST-mediated activation of Nitrate Reductase 1.2 in rice. Mol. Plant **15**:167–178.

Heinemann, B., Künzler, P., Eubel, H., Braun, H.P., and Hildebrandt, T.M. (2021). Estimating the number of protein molecules in a plant cell: protein and amino acid homeostasis during drought. Plant Physiol. **185**:385–404.

Heredia, M.C., Kant, J., Prodhan, M.A., Dixit, S., and Wissuwa, M. (2022). Breeding rice for a changing climate by improving adaptations to water saving technologies. Theor. Appl. Genet. **135**:17–33.

Hiei, Y., Ohta, S., Komari, T., and Kumashiro, T. (1994). Efficient transformation of rice (*Oryza sativa L.*) mediated by Agrobacterium and sequence analysis of the boundaries of the T-DNA. Plant J. **6**:271–282.

Hoosbeek, M.R., Li, Y., and Scarascia-Mugnozza, G.E. (2006). Free atmospheric CO2 enrichment (FACE) increased labile and total carbon in the mineral soil of a short rotation *Poplar* plantation. Plant Soil **281**:247–254.

Hu, B., Wang, W., Chen, J., Liu, Y., and Chu, C. (2023). Genetic improvement toward nitrogen-use efficiency in rice: Lessons and perspectives. Mol. Plant **16**:64–74.

Ingargiola, C., Jéhanno, I., Forzani, C., Marmagne, A., Broutin, J., Clément, G., Leprince, A.S., and Meyer, C. (2023). The *Arabidopsis* Target of Rapamycin kinase regulates ammonium assimilation and glutamine metabolism. Plant Physiol. **192**:2943–2957.

James, D., Borphukan, B., Fartyal, D., Ram, B., Singh, J., Manna, M., Sheri, V., Panditi, V., Yadav, R., Achary, V.M.M., and Reddy, M.K. (2018). Concurrent Overexpression of *OsGS1;1* and *OsGS2* Genes in Transgenic Rice (Oryza sativa L.): Impact on Tolerance to Abiotic Stresses. Front. Plant Sci. **9**:786.

Ji, Y., Huang, W., Wu, B., Fang, Z., and Wang, X. (2020). The amino acid transporter AAP1 mediates growth and grain yield by regulating neutral amino acid uptake and reallocation in *Oryza sativa*. J. Exp. Bot. **71**:4763–4777.

Kantidakis, T., Ramsbottom, B.A., Birch, J.L., Dowding, S.N., and White, R.J. (2012). mTOR associates with TFIIIC, is found at tRNA and 5S rRNA genes, and targets their repressor Maf1 (vol 107, pg 11823, 2010). Proc. Natl. Acad. Sci. USA **109**:11465.

Kawaguchi, R., Williams, A.J., Bray, E.A., and Bailey-Serres, J. (2003). Water-deficit-induced translational control in *Nicotiana tabacum*. Plant Cell Environ. **26**:221–229.

Kawaguchi, R., Girke, T., Bray, E.A., and Bailey-Serres, J. (2004). Differential mRNA translation contributes to gene regulation under non-stress and dehydration stress conditions in *Arabidopsis thaliana*. Plant J. **38**:823–839.

Khanna, A., Pradhan, A., and Curran, S.P. (2015). Emerging Roles for Maf1 beyond the Regulation of RNA Polymerase III Activity. J. Mol. Biol. **427**:2577–2585.

Kim, J., and Guan, K.L. (2019). mTOR as a central hub of nutrient signalling and cell growth. Nat. Cell Biol. **21**:63–71.

Lee, D.H., Park, S.J., Ahn, C.S., and Pai, H.S. (2017). *MRF* Family Genes Are Involved in Translation Control, Especially under Energy-Deficient Conditions, and Their Expression and Functions Are Modulated by the TOR Signaling Pathway. Plant Cell **29**:2895–2920.

Léran, S., Edel, K.H., Pervent, M., Hashimoto, K., Corratgé-Faillie, C., Offenborn, J.N., Tillard, P., Gojon, A., Kudla, J., and Lacombe, B. (2015). Nitrate sensing and uptake in *Arabidopsis* are enhanced by ABI2, a phosphatase inactivated by the stress hormone abscisic acid. Sci. Signal. **8**:ra43.

Li, C., Salas, W., DeAngelo, B., and Rose, S. (2006). Assessing alternatives for mitigating net greenhouse gas emissions and increasing yields from rice production in China over the next twenty years. J. Environ. Qual. **35**:1554–1565.

Li, C., Tang, Z., Wei, J., Qu, H., Xie, Y., and Xu, G. (2016). The *OsAMT1.1* gene functions in ammonium uptake and ammonium-potassium homeostasis over low and high ammonium concentration ranges. J. Genet. Genomics **43**:639–649.

Li, L., Liu, K.H., and Sheen, J. (2021). Dynamic Nutrient Signaling Networks in Plants. Annu. Rev. Cell Dev. Biol. **37**:341–367.

Li, Y.L., Fan, X.R., and Shen, Q.R. (2008). The relationship between rhizosphere nitrification and nitrogen-use efficiency in rice plants. Plant Cell Environ. **31**:73–85.

Liu, G.Y., and Sabatini, D.M. (2020). mTOR at the nexus of nutrition, growth, ageing and disease. Nat. Rev. Mol. Cell Biol. **21**:183–203.

Liu, H., Ding, Y., Zhou, Y., Jin, W., Xie, K., and Chen, L.L. (2017). CRISPR-P 2.0: An Improved CRISPR-Cas9 Tool for Genome Editing in Plants. Mol. Plant **10**:530–532.

Liu, Q., Wu, K., Song, W., Zhong, N., Wu, Y., and Fu, X. (2022a). Improving Crop Nitrogen Use Efficiency Toward Sustainable Green Revolution. Annu. Rev. Plant Biol. **73**:523–551.

Liu, X., Hu, B., and Chu, C. (2022b). Nitrogen assimilation in plants: current status and future prospects. J. Genet. Genomics **49**:394–404.

Liu, Y., Duan, X., Zhao, X., Ding, W., Wang, Y., and Xiong, Y. (2021). Diverse nitrogen signals activate convergent ROP2-TOR signaling in *Arabidopsis*. Dev. Cell **56**:1283–1295.e5.

Luo, L.J. (2010). Breeding for water-saving and drought-resistance rice (WDR) in China. J. Exp. Bot. **61**:3509–3517.

Mahfouz, M.M., Kim, S., Delauney, A.J., and Verma, D.P.S. (2006). *Arabidopsis* TARGET OF RAPAMYCIN interacts with RAPTOR, which regulates the activity of S6 kinase in response to osmotic stress signals. Plant Cell **18**:477–490.

Mallén-Ponce, M.J., Pérez-Pérez, M.E., and Crespo, J.L. (2022). Analyzing the impact of autotrophic and heterotrophic metabolism on the nutrient regulation of TOR. New Phytol. **236**:1261–1266.

Matsuura, H., Takenami, S., Kubo, Y., Ueda, K., Ueda, A., Yamaguchi, M., Hirata, K., Demura, T., Kanaya, S., and Kato, K. (2013). A Computational and Experimental Approach Reveals that the 5 ’-Proximal Region of the 5 ’-UTR has a Cis-Regulatory Signature Responsible for Heat Stress-Regulated mRNA Translation in *Arabidopsis*. Plant Cell Physiol. **54**:474–483.

Meng, Y., Zhang, N., Li, J., Shen, X., Sheen, J., and Xiong, Y. (2022). TOR kinase, a GPS in the complex nutrient and hormonal signaling networks to guide plant growth and development. J. Exp. Bot. **73**:7041–7054.

Merchante, C., Stepanova, A.N., and Alonso, J.M. (2017). Translation regulation in plants: an interesting past, an exciting present and a promising future. Plant J. **90**:628–653.

Merret, R., Nagarajan, V.K., Carpentier, M.C., Park, S., Favory, J.J., Descombin, J., Picart, C., Charng, Y.Y., Green, P.J., Deragon, J.M., and Bousquet-Antonelli, C. (2015). Heat-induced ribosome pausing triggers mRNA co-translational decay in *Arabidopsis thaliana*. Nucleic Acids Res. **43**:4121–4132.

Michels, A.A. (2011). MAF1: a new target of mTORC1. Biochem. Soc. Trans. **39**:487–491.

Nguyen, T., Mills, J.C., and Cho, C.J. (2023). The coordinated management of ribosome and translation during injury and regeneration. Front. Cell Dev. Biol. **11**, 1186638.

Nojiri, Y., Kaneko, Y., Azegami, Y., Shiratori, Y., Ohte, N., Senoo, K., Otsuka, S., and Isobe, K. (2020). Dissimilatory Nitrate Reduction to Ammonium and Responsible Microbes in Japanese Rice Paddy Soil. Microb. Environ. **35**, ME20069.

O’Leary, B.M., Oh, G.G.K., Lee, C.P., and Millar, A.H. (2020). Metabolite Regulatory Interactions Control Plant Respiratory Metabolism via Target of Rapamycin (TOR) Kinase Activation. Plant Cell **32**:666–682.

Oliveira Andrade, M., Sforça, M.L., Batista, F.A.H., Figueira, A.C.M., and Benedetti, C.E. (2020). The MAF1 Phosphoregulatory Region Controls MAF1 Interaction with the RNA Polymerase III C34 Subunit and Transcriptional Repression in Plants. Plant Cell **32**:3019–3035.

Ouyang, J., Cai, Z., Xia, K., Wang, Y., Duan, J., and Zhang, M. (2010). Identification and analysis of eight peptide transporter homologs in rice. Plant Sci. **179**:374–382.

Ouyang, W., Struik, P.C., Yin, X., and Yang, J. (2017). Stomatal conductance, mesophyll conductance, and transpiration efficiency in relation to leaf anatomy in rice and wheat genotypes under drought. J. Exp. Bot. **68**:5191–5205.

Ren, M., Venglat, P., Qiu, S., Feng, L., Cao, Y., Wang, E., Xiang, D., Wang, J., Alexander, D., Chalivendra, S., et al. (2012). Target of rapamycin signaling regulates metabolism, growth, and life span in *Arabidopsis*. Plant Cell **24**:4850–4874.

Sanders, A., Collier, R., Trethewy, A., Gould, G., Sieker, R., and Tegeder, M. (2009). AAP1 regulates import of amino acids into developing *Arabidopsis* embryos. Plant J. **59**:540–552.

Scarpin, M.R., Leiboff, S., and Brunkard, J.O. (2020). Parallel global profiling of plant TOR dynamics reveals a conserved role for LARP1 in translation. Elife **9**, e58795.

Scarpin, M.R., Simmons, C.H., and Brunkard, J.O. (2022). Translating across kingdoms: target of rapamycin promotes protein synthesis through conserved and divergent pathways in plants. J. Exp. Bot. **73**:7016–7025.

Schepetilnikov, M., and Ryabova, L.A. (2018). Recent discoveries on the role of TOR (Target of Rapamycin) signaling in translation in plants. Plant Physiol. **176**:1095–1105.

Sun, L., Yu, Y., Hu, W., Min, Q., Kang, H., Li, Y., Hong, Y., Wang, X., and Hong, Y. (2016). Ribosomal protein S6 kinase1 coordinates with TOR-Raptor2 to regulate thylakoid membrane biosynthesis in rice. Biochim. Biophys. Acta **1861**:639–649.

Tegeder, M., and Masclaux-Daubresse, C. (2018). Source and sink mechanisms of nitrogen transport and use. New Phytol. **217**:35–53.

Tran, T.T., Kano-Nakata, M., Takeda, M., Menge, D., Mitsuya, S., Inukai, Y., and Yamauchi, A. (2014). Nitrogen application enhanced the expression of developmental plasticity of root systems triggered by mild drought stress in rice. Plant Soil **378**:139–152.

Waadt, R., Seller, C.A., Hsu, P.K., Takahashi, Y., Munemasa, S., and Schroeder, J.I. (2022). Plant hormone regulation of abiotic stress responses. Nat. Rev. Mol. Cell Biol. **23**:680–694.

Wang, L., Li, H., Zhao, C., Li, S., Kong, L., Wu, W., Kong, W., Liu, Y., Wei, Y., Zhu, J.K., and Zhang, H. (2017). The inhibition of protein translation mediated by AtGCN1 is essential for cold tolerance in *Arabidopsis thaliana*. Plant Cell Environ. **40**:56–68.

Wang, M.Y., Siddiqi, M.Y., Ruth, T.J., and Glass, A. (1993). Ammonium Uptake by Rice Roots (II. Kinetics of $13NH_4^+$ Influx across the Plasmalemma). Plant Physiol. **103**:1259–1267.

Wang, M.Y., Glass, A.D.M., Shaff, J.E., and Kochian, L.V. (1994). Ammonium Uptake by Rice Roots .3. Electrophysiology. Plant Physiol. **104**:899–906.

Wang, P., Zhao, Y., Li, Z., Hsu, C.C., Liu, X., Fu, L., Hou, Y.J., Du, Y., Xie, S., Zhang, C., et al. (2018). Reciprocal Regulation of the TOR Kinase and ABA Receptor Balances Plant Growth and Stress Response. Mol. Cell **69**:100–112.e6.

Willis, I.M., and Moir, R.D. (2007). Integration of nutritional and stress signaling pathways by Maf1. Trends Biochem. Sci. **32**:51–53.

Wu, X., Xie, X., Yang, S., Yin, Q., Cao, H., Dong, X., Hui, J., Liu, Z., Jia, Z., Mao, C., and Yuan, L. (2022). OsAMT1;1 and OsAMT1;2 Coordinate Root Morphological and Physiological Responses to Ammonium for Efficient Nitrogen Foraging in Rice. Plant Cell Physiol. **63**:1309–1320.

Xia, H., Zhang, X., Liu, Y., Bi, J., Ma, X., Zhang, A., Liu, H., Chen, L., Zhou, S., Gao, H., et al. (2022). Blue revolution for food security under carbon neutrality: A case from the water-saving and drought-resistance rice. Mol. Plant **15**:1401–1404.

Xiong, Y., McCormack, M., Li, L., Hall, Q., Xiang, C., and Sheen, J. (2013). Glucose-TOR signalling reprograms the transcriptome and activates meristems. Nature **496**:181–186.

Xiong, Y., and Sheen, J. (2012). Rapamycin and glucose-target of rapamycin (TOR) protein signaling in plants. J. Biol. Chem. **287**:2836–2842.

Xu, Z.Z., and Zhou, G.S. (2006). Combined effects of water stress and high temperature on photosynthesis, nitrogen metabolism and lipid peroxidation of a perennial grass Leymus chinensis. Planta **224**:1080–1090.

Yang, X., Li, Y., Ren, B., Ding, L., Gao, C., Shen, Q., and Guo, S. (2012). Drought-induced root aerenchyma formation restricts water uptake in rice seedlings supplied with nitrate. Plant Cell Physiol. **53**:495–504.

Ye, R., Wang, M., Du, H., Chhajed, S., Koh, J., Liu, K.H., Shin, J., Wu, Y., Shi, L., Xu, L., et al. (2022). Glucose-driven TOR-FIE-PRC2 signalling controls plant development. Nature **609**:986–993.

Yu, S., Ali, J., Zhou, S., Ren, G., Xie, H., Xu, J., Yu, X., Zhou, F., Peng, S., Ma, L., et al. (2022). From Green Super Rice to green agriculture: Reaping the promise of functional genomics research. Mol. Plant **15**:9–26.

Zhang, H., Zhu, J., Gong, Z., and Zhu, J.K. (2022a). Abiotic stress responses in plants. Nat. Rev. Genet. **23**:104–119.

Zhang, X., Sun, H., Bi, J., Yang, B., Zhang, J., Wang, C., and Zhou, S. (2022b). Estimate greenhouse gas emissions from water-saving and drought-resistance rice paddies by deNitrification-deComposition model. Clean Technol. Envir. **24**:161–171.

Zhong, C., Cao, X., Hu, J., Zhu, L., Zhang, J., Huang, J., and Jin, Q. (2017). Nitrogen Metabolism in Adaptation of Photosynthesis to Water Stress in Rice Grown under Different Nitrogen Levels. Front. Plant Sci. **8**:1079.

Molecular Plant, Volume *17*

Supplemental information

Mitigating growth-stress tradeoffs via elevated TOR signaling in rice

Wei Li, Jiaqi Liu, Zeqi Li, Ruiqiang Ye, Wenzhen Chen, Yuqing Huang, Yue Yuan, Yi Zhang, Huayi Hu, Peng Zheng, Zhongming Fang, Zeng Tao, Shiyong Song, Ronghui Pan, Jian Zhang, Jumim Tu, Jen Sheen, and Hao Du

Supplemental Information

Supplemental Figures

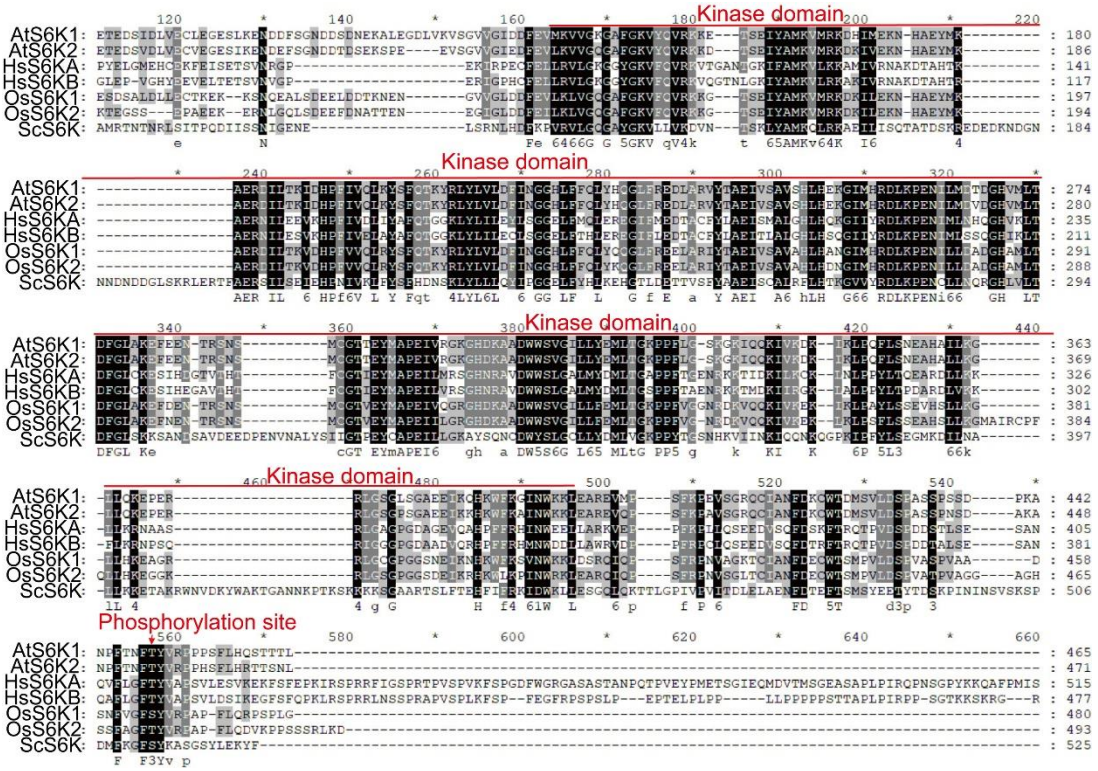

Supplemental Figure 1. Comparison of S6K protein sequences.

Arabidopsis AtS6K (AtS6K1, At3g08730 and AtS6K2, At3g08720), *Oryza sativa* OsS6K (OsS6K1, Os03g0334000), and OsS6K2, Os07g0680900), *Homo sapiens* HsS6K (HsS6KA, P23443.2, and HsS6KB, Q9UBS0.2), and *Saccharomyces cerevisiae* ScS6K (YPK3, P38070.1) protein sequences were aligned by Clustal W. Jalview multiple alignment editor programswere employed to generate the picture. The level of conservation is represented by a color code in which the most conserved residues are in black, those with intermediate conservation are in gray and the least conserved are in white.

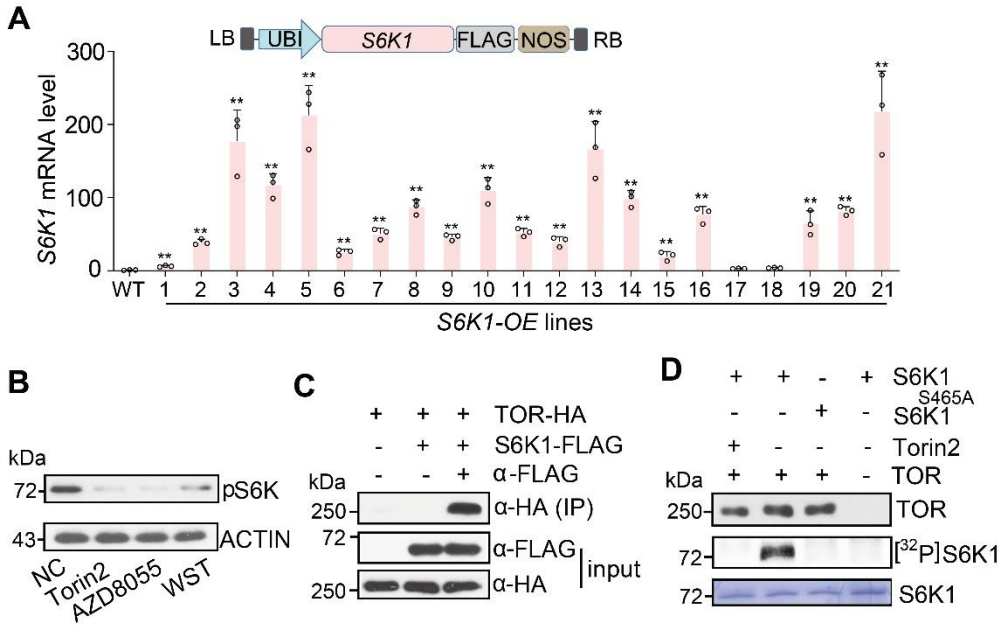

Supplemental Figure 2. Evaluation of the effect of WST on rice and characterization of rice S6K1.

(A) Schematic construct diagram and relative mRNA level of rice *S6K1* overexpression lines by qRT-PCR. Error bars indicate means ± SD (n = 3). Statistical significance was assessed using two-tailed t-tests. ***P* < 0.01 (t-test).

(B) WST represses TOR activity *in vivo*. TOR activation is detected using an anti-phospho antibody to S6K1, protein from wild-type rice detected by anti-FLAG antibody after treatment. The upper band indicates phosphorylated S6K1. 10 μM TOR inhibitors (Torin 2, AZD8055) were spread on the leaves of 28-day rice for 7 days, sampled at 35 DAG.

(C) TOR interacts with S6K1 *in vivo*. Co-immunoprecipitation (Co-IP) of FLAG-tagged S6K1 with HA-tagged TOR expressed in rice protoplasts. Co-immunoprecipitation (Co-IP) of TOR with S6K1. FLAG-tagged S6K1 with HA-tagged TOR were expressed in rice protoplasts. Total protoplast proteins were immunoprecipitated with anti-HA antibody-conjugated resin, and the coimmunoprecipitate was detected using the anti-FLAG antibody.

(D) TOR phosphorylates rice S6K1 protein *in vitro*.

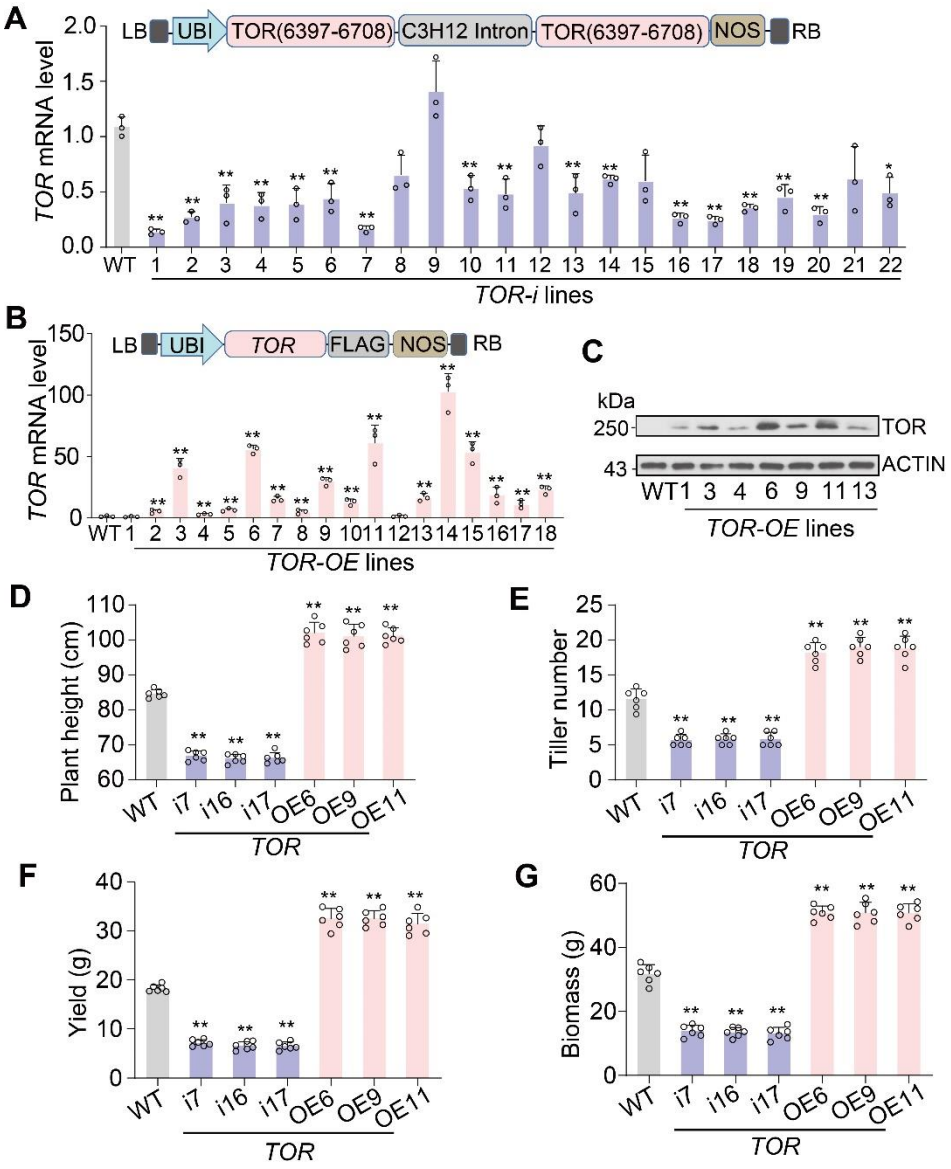

Supplemental Figure 3. Creation of *TOR* transgenic rice.

(A) Schematic construct diagram and relative mRNA level of rice *TOR* RNA interference (*TOR-i*) lines by qRT-PCR (quantitative real-time PCR). Error bars indicate means ± SD (n = 3). Statistical significance was assessed using two-tailed t-tests. **P* < 0.05 (t-test), ***P* < 0.01 (t-test).

(B) *TOR* overexpression (OE) construct diagram (B), LB, left border; RB, right border, three FLAG tag fused at C-terminal, and relative mRNA level of *TOR* in *TOR* transgenic lines and WT examined by qRT-PCR. Error bars indicate means ± SD (n = 3). Statistical significance was assessed using two-tailed t-tests. ***P* < 0.01 (t-test).

(C) *TOR* overexpression lines were confirmed by immunoblot analyses.

(D-G) Statistical data on plant height (D), tiller number (E), yield (F), and biomass (G) of *TOR* transgenic lines. Error bars indicate means ±SD (n = 6). Statistical significance was assessed using two-tailed t-tests. ***P* < 0.01 (t-test).

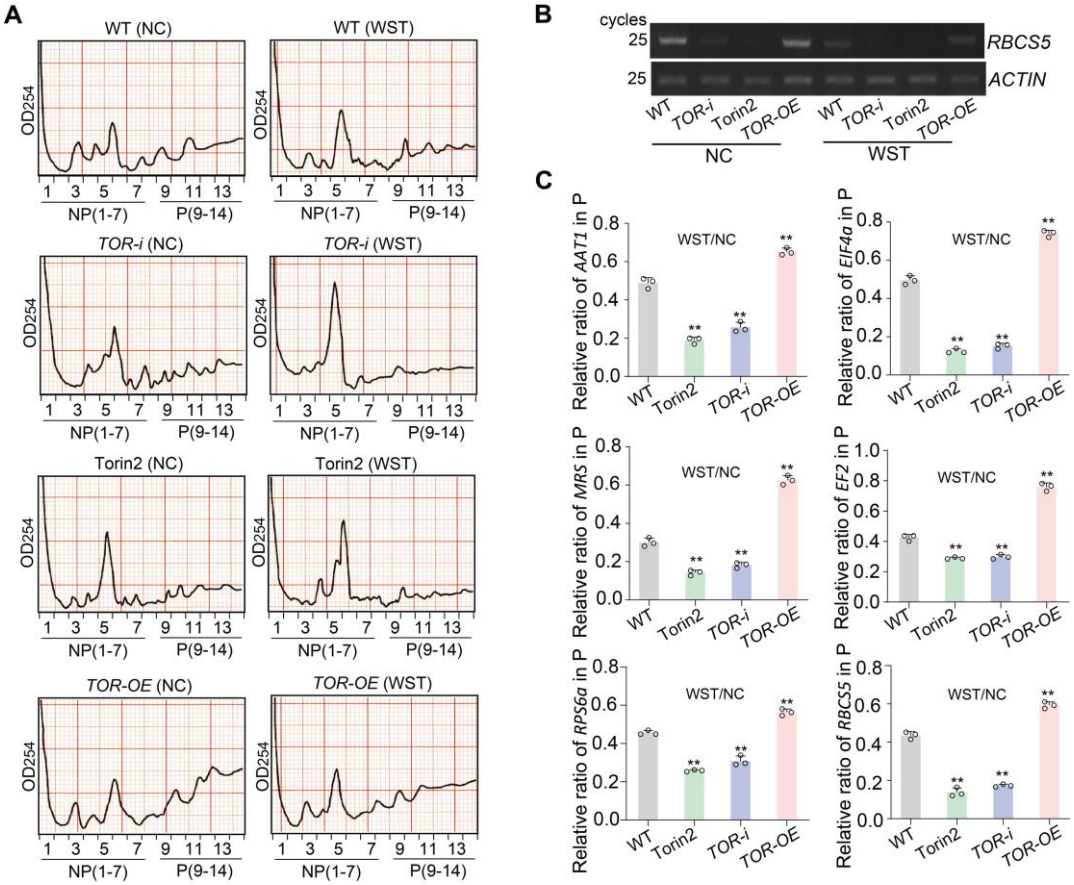

Supplemental Figure 4. Polysome profiles analysis of rice seedlings under NC and WST.

(A) Polysome profiles analysis of rice in normal conditions (NC) or water-saving treatment (WST), 10 μM torin2 and *TOR* transgenic lines. Plant materials and growth conditions were described in this method.

(B) RT-PCR analysis of *RBCS5* expression levels in total mRNA was extracted from quantified polysomal (P) mRNA. *ACTIN* was used as an internal control.

(C) Bar graph shows the ratio of the specific mRNAs in polysomal (P) mRNA. Total mRNA was extracted from polysomal (P) mRNA, followed by cDNA synthesis and qRT-PCR using gene-specific primers. The abundance of specific mRNA in polysomal (P) mRNA was quantified as a relative level in P using *ACTIN* as a reference gene.

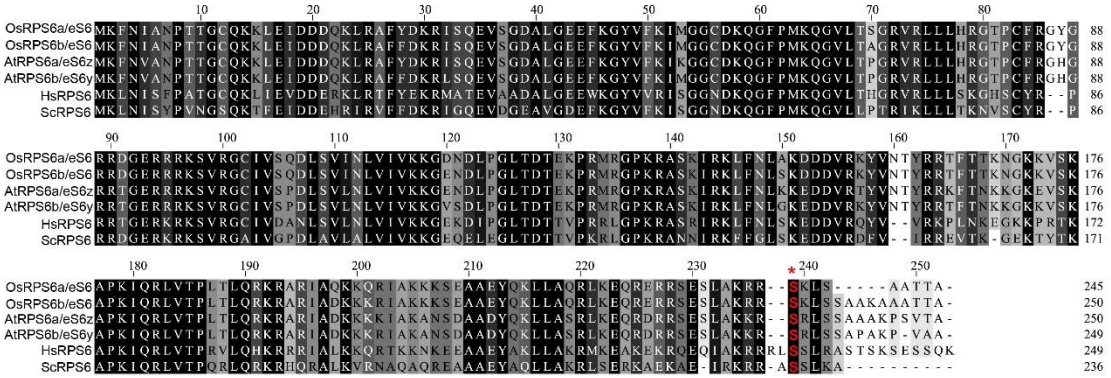

Supplemental Figure 5. Comparison of RPS6 amino acid sequences. *Arabidopsis* RPS6s (AtRPS6A/es6z, At4g31700, and AtRPS6B/es6y, At5g10360), *Oryza sativa* RPS6s (OsRPS6a/es6, Os03g0390000, and OsRPS6b/es6, Os07g0622100), *Homo sapiens* RPS6 (HsRPS6, NP_001001.2), and *Saccharomyces cerevisiae* RPS6 (ScRPS6, NP_015235.1) protein sequences were aligned by Clustal W. Jalview multiple alignment editor programswere employed to generate the picture. The level of conservation is represented by a color code in which the most conserved residues are in black, those with intermediate conservation are gray and the least conserved are in white. The asterisk indicates a conserved phosphorylation site detected by commercial antibody pRPS6a-Ser237 (Agrisera, AS194291).

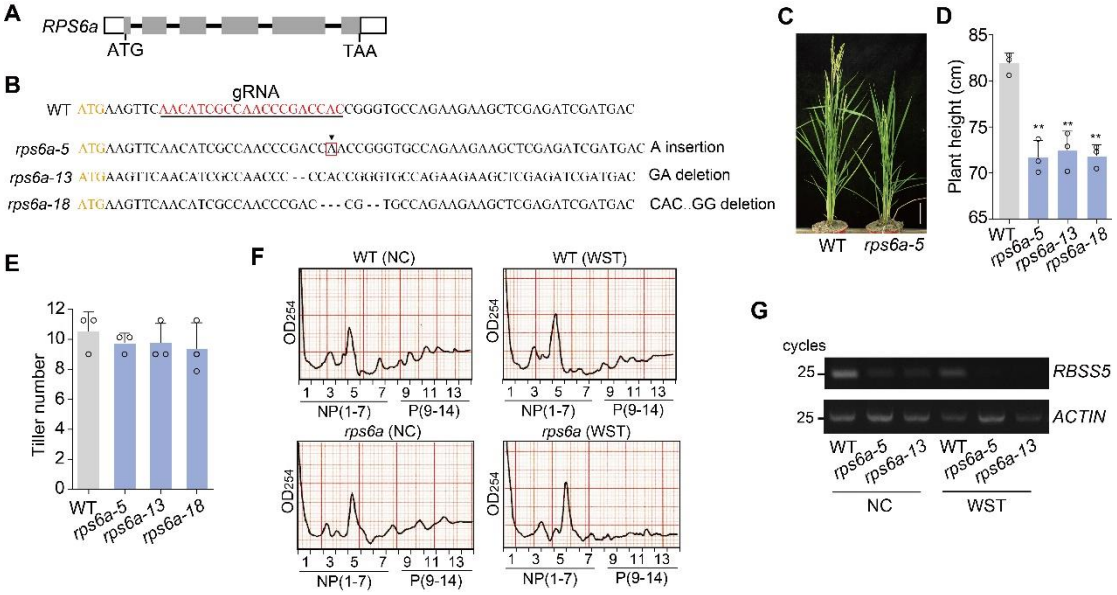

Supplemental Figure 6. Identification and analyses of rice *rps6a* mutants.

(A) Diagrammatic presentation of rice *RPS6a*/es6 and mutant *rps6a*, the gray box indicates the exons and the black line indicates the introns.

(B) Diagram for the sequence of rice *rps6a* mutants created by CRISPR/Cas9 system.

(C-E) Performance (C), plant height (D) and tiller number (E) of WT and *rps6a* mutants at reproductive stage. Scale bars, 10 cm. Error bars indicate means ± SD (n = 3). Statistical significance was assessed using two-tailed t-tests. $^{**}P < 0.01$ (t-test).

(F) Polysome profiles analysis of WT and *rps6a* mutants under normal conditions (NC) or water-saving treatment (WST).

(G) RT-PCR analysis of *RbcS5* expression level in total mRNA was extracted from quantified polysomal (P) mRNA. *ACTIN* was used as an internal control.

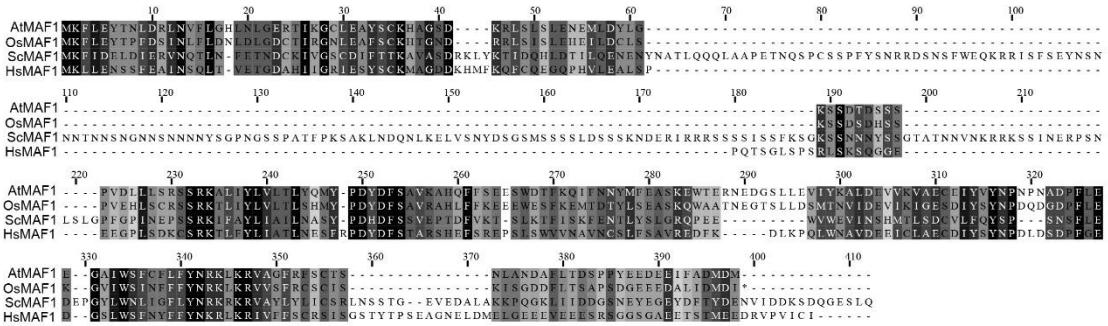

Supplemental Figure 7. Comparison of MAF1 protein sequences.

Arabidopsis AtMAF1 (KAG7602094.1), *Oryza sativa* OsMAF1 (XP_015636424.1), *Saccharomyces cerevisiae* ScMAF1 (AJU85789.1), and *Homo sapiens* HsMAF1 (NP_115648.2) protein sequences were aligned by Clustal W. Jalview multiple alignment editor programswere employed to generate the picture. The level of conservation is represented by a color code in which the most conserved residues are in black, those with intermediate conservation are gray and the least conserved are in white.

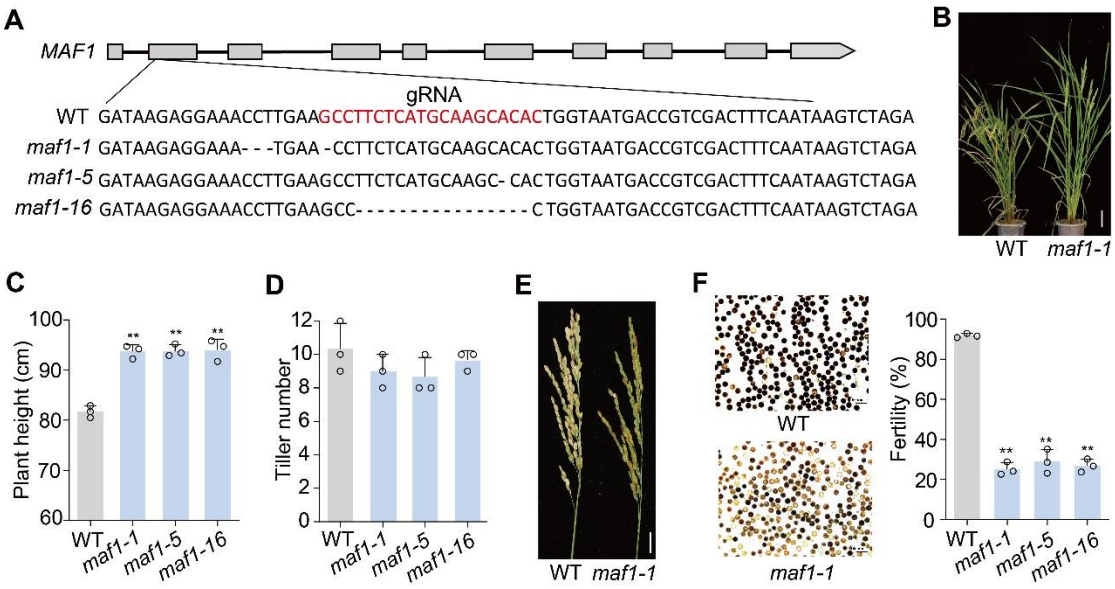

Supplemental Figure 8. Phenotypic analysis of rice *maf1* mutants.

(A) Diagrammatic presentation of rice *MAF1* and the *maf1* mutants, the gray box indicates the intron, the black line indicates the exon, the red sequence is the gRNA target, and the short broken line indicates nucleotide deletion in rice *maf1* mutants.

(B-D) Performance (B) and plant height (C) and tiller number (D) of WT and *maf1* mutants at reproductive stage. Scale bars, 10 cm. Error bars indicate means ± SD (n = 3). Statistical significance was assessed using two-tailed t-tests. ***P* < 0.01 (t-test).

(E) The performance of panicle and primary branches of WT and *maf1* mutant in the field. Scale bars, 1 cm.

(F) KI-I_2 staining of pollen from WT and *maf1* mutants. Error bars indicate means ± SD (n = 3). Statistical significance was assessed using two-tailed t-tests. ***P* < 0.01 (t-test).

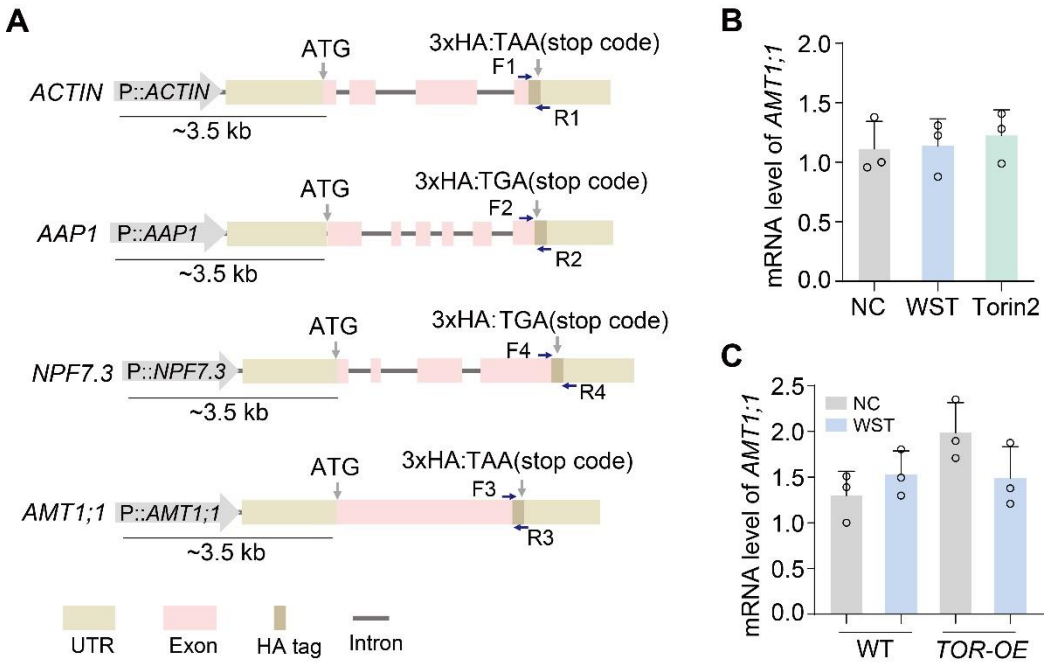

Supplemental Figure 9. TOR signaling regulates the translation of AAP1, NPF7.3 and AMT1;1 under WST.

(A) Schematic illustration of constructs of genome DNA with HA fused expression vectors of *ACTIN*, *AAP1*, *NPF7.3* and *AMT1.1* for rice protoplast transformation.

(B and C) qRT-PCR assays of transcripts of *AMT1;1* from WT with different treatments (B), and *TOR-OE* rice under NC and WST (C) at seedling stage of 35 DAG.

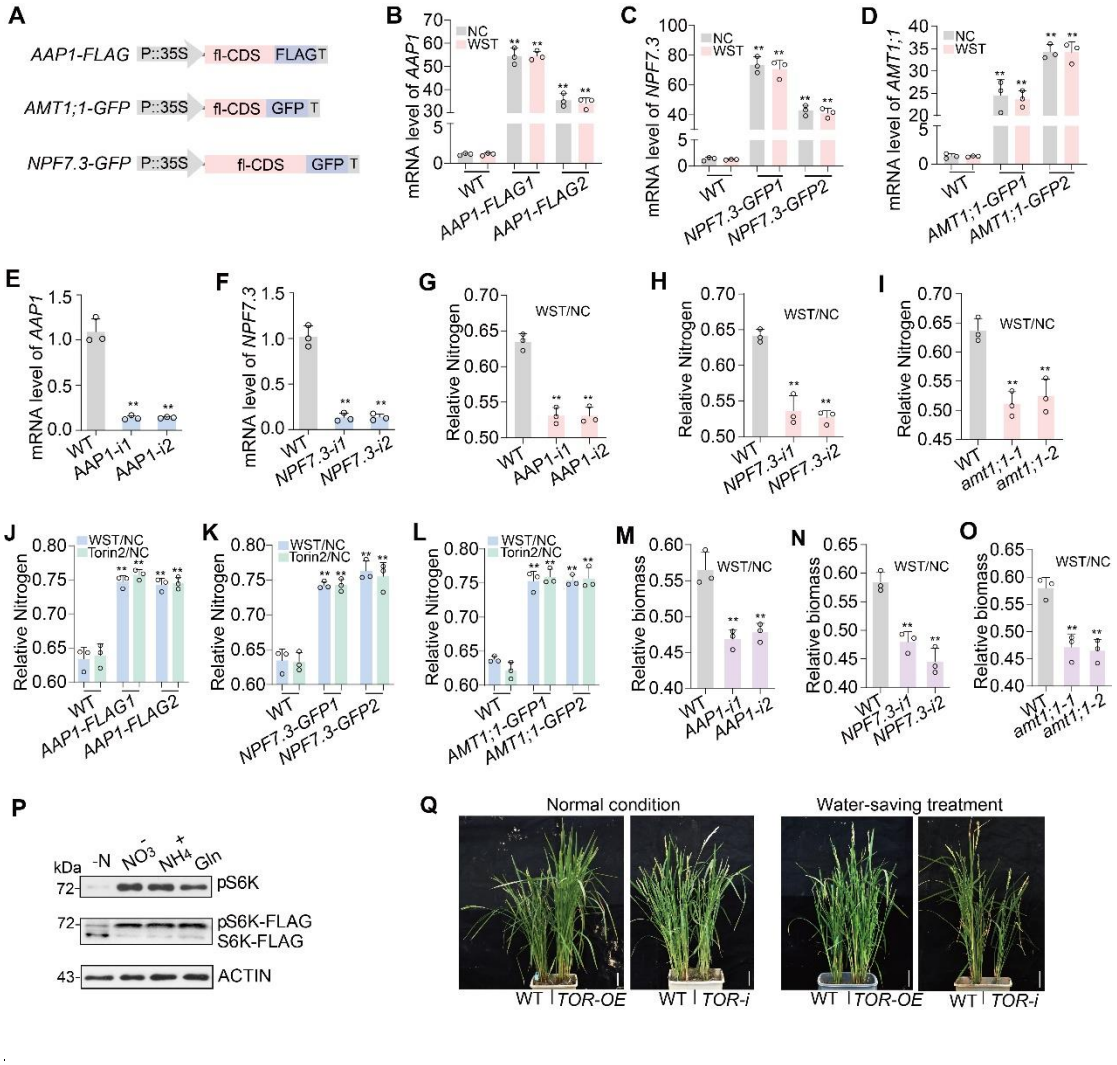

Supplemental Figure 10. Rice AAP1, NPF7.3 and AMT1;1 are involved in growth productivity under WST.

(A) Schematic illustration of constructs for full-length CDS with tag-fused overexpression vectors for generating transgenic rice.

(B-D) qRT-PCR assay of the mRNA level of *AAP1* (B), *NPF7.3* (C) and *AMT1;1* (D) in transgenic rice containing the above constructs in (A) under NC and WST, WT as *ZhongHua11*. Error bars indicate means ± SD (n = 3). Statistical significance was assessed using two-tailed t-tests. ***P* < 0.01 (t-test).

(E and F) qRT-PCR assay of the mRNA level of *AAP1* (E) and *NPF7.3* (F) in *AAP1* and *NPF7.3* RNA interference rice, respectively, WT as *ZhongHua11*. Error bars indicate means ± SD (n = 3). Statistical significance was assessed using two-tailed t-tests. ***P* < 0.01 (t-test).

(G-I) Relative nitrogen content in rice seedlings of RNA interference lines *AAP1-i* (G), *NPF7.3-i* (H) and *AMT1;1* knocked out mutants (I) at DAG 35 under NC and WST. Error bars indicate means ± SD (n = 3). Statistical significance was assessed using two-tailed t-tests. ***P* < 0.01 (t-test).

(J-L) Statistical data of relative nitrogen content in transgenic lines *AAP1-FLAG* (D), *NPF7.3-GFP* (E) and *AMT1;1-GFP* (F) at 35 DAG after treatments with WST and Torin2. Error bars indicate means ± SD (n = 3). Statistical significance was assessed using two-tailed t-tests. ***P* < 0.01 (t-test).

(M-O) Statistical data of relative above-ground biomass in RNA interference lines *AAP1-I* (M), *NPF7.3-i* (N) and *AMT1;1* knocked out mutants (O) at DAG 35 under NC and WST. Error bars indicate means ± SD (n = 3). Statistical significance was assessed using two-tailed t-tests. ***P* < 0.01 (t-test).

(P) Nitrate, ammonium, and Gln activate TOR kinase in normal conditions by immunoblot analyses using *S6K1* transgenic rice. Sodium nitrate (NO_3^-, 50 mM), ammonium succinate (NH_4^+, 50 mM), or Gln (50 mM).

(Q) Performance of *TOR* transgenic rice under WST at reproductive stage. Scale bars, 10 cm.

Supplemental Tables

Supplemental Table 1. A list of all primers used in this study.

Supplemental Table 2. RNA_seq data from ribosome profiling in this study.

Supplemental Table 3. Raw data in this study.